Topology Optimization of 3D Printed Concrete Beams: A Study of Strength to Weight Ratios

M.Tech. Thesis

By

PRINCE KUMAR

(2302104008)

DEPARTMENT OF CIVIL ENGINEERING

INDIAN INSTITUTE OF TECHNOLOGY INDORE

May 2025

Topology Optimization of 3D Printed Concrete Beams: A Study of Strength to Weight Ratios

A THESIS

Submitted in partial fulfillment of the requirements for the award of the degree
of

Master of Technology
(2023-2025)
STRUCTURAL ENGINEERING

By
PRINCE KUMAR
(2302104008)
Under Guidance
of
Dr. Abhishek Rajput
(Associate Professor)

DEPARTMENT OF CIVIL ENGINEERING

INDIAN INSTITUTE OF TECHNOLOGY INDORE

May 2025

INDIAN INSTITUTE OF TECHNOLOGY INDORE

CANDIDATE'S DECLARATION

I hereby certify that the work which is being presented in the thesis entitled **TOPOLOGY OPTIMIZATION OF 3D PRINTED CONCRETE BEAMS: A STUDY OF STRENGTH TO WEIGHT RATIOS** in the partial fulfillment of the requirements for the award of the degree of **MASTER OF TECHNOLOGY** and submitted in the **DEPARTMENT OF CIVIL ENGINEERING, INDIAN INSTITUTE OF TECHNOLOGY INDORE**, is an authentic record of my own work carried out during the time period from **JUNE 2023** to **MAY 2025** under the supervision of Dr. Abhishek Rajput, Associate Professor, Department of Civil Engineering, Indian Institute of Technology, Indore.

The matter presented in this thesis has not been submitted by me for the award of any other degree of this or any other institute.

Prince Kumar
Date: 23/05/2025

This is to certify that the above statement made by the candidate is correct to the best of my/our knowledge.

Signature of the Supervisor of M.Tech. Thesis
Dr. Abhishek Rajput
Date:

Prince Kumar has successfully given his M.Tech. Oral Examination held on **9 May 2025**.

Signature of Supervisor of M.Tech. Thesis
Date:

Convener, DPCG
Date: May 27, 2025

ACKNOWLEDGEMENTS

ABSTRACT

The construction industry is a major contributor to global energy consumption and CO_2 emissions, necessitating material-efficient design solutions aligned with green building standards such as IGBC and GRIHA. This thesis explores the integration of topology optimization with 3D concrete printing (3DCP) to design and fabricate optimized concrete beams that achieve superior strength-to-weight ratios while minimizing material usage. A concrete beam of dimensions 500 mm $\times$ 100 mm $\times$ 20 mm was optimized using ANSYS Workbench for minimum compliance, and the resulting design was traced and adapted for 3D printing. A suitable 3D printable concrete mix was developed through trial-and-error, ensuring essential properties like buildability and extrudability. The study further compares the structural performance of topology-optimized beams against beams with alternative infill patterns (S-shaped and N-shaped) and conventional mould-cast beams. Experimental validation involved four-point flexural tests to assess failure loads, deflection behaviour, and material efficiency. Results indicate that the topology-optimized 3DCP beam achieved an 8.04% improvement in strength-to-weight ratio compared to conventional beams, demonstrating the viability of combining computational design tools with advanced manufacturing techniques. This research highlights the potential of topology optimization in enhancing the sustainability of concrete structures by reducing material use without compromising structural integrity. The findings underscore the role of commercial FEA tools, such as ANSYS, in facilitating optimized designs compatible with 3DCP technology, paving the way for greener, more efficient construction practices.

LIST OF CONTENTS

LIST OF FIGURES

LIST OF TABLES

Chapter 1

Introduction

1.1 Overview

Environmental degradation has been a major cause of concern since industrial revolution. In the latest report of (Global Status Report for Buildings and Construction 2024/2025 | UNEP - UN Environment Programme) (UNEP) published by UN Environment programme and the (Global Status Report | GlobalABC) Global Alliance for Buildings and Construction (GlobalABC), states that construction sector consumes 32 per cent of global energy and contribute to 34 per cent of global CO_2.

With growing urgency of reducing CO_2 in the environment, it has been an important criteria for structural engineers to implement material efficiency in the design of structural members. One such method to reduce the material consumption is topology optimization. As the construction industry prioritizes sustainability, complying with the latest standards from the Indian Green Building Council (IGBC | IGBC Green New Buildings Rating System) and GRIHA (Green Rating for Integrated Habitat Assesment) has become essential to reducing carbon footprints. Topology optimization in 3D printable concrete beams offers an innovative approach to cutting cement use, thus contributing to improved sustainability ratings. This aligns with the green building goals of IGBC and GRIHA, which emphasize material efficiency and minimizing environmental impact.

Integrating topology optimization with 3D printing is need of the hour. There are various finite element based software's that has tools, which use the mathematical models to optimize objects and reduce its weight. Ansys is one of the software that can help designers to optimize beams. Earlier due to manufacturability constraints, such beams could not be constructed, as formwork for such a beam would be complex and time consuming. With the advent of 3D concrete printer, it is possible to print such a beam. In this study, it has been demonstrated how one can design an optimized beam and print it using 3D concrete printer.

1.2 Introduction to Topology optimization

Topology optimization is a design technique that leverages advanced computational algorithms to determine the most efficient material distribution within a defined design space. This method optimizes structures to meet specific performance objectives, such as maximizing stiffness or minimizing material usage, while adhering to necessary constraints like strength and functionality. It originated in engineering fields like aerospace and automotive design but has found applications in civil engineering, particularly for optimizing structural components such as beams, columns, and trusses.

The process of topology optimization involves creating a virtual design space, within which material is redistributed based on the analysis of various loading conditions (Deaton and Grandhi 2014). The goal is to eliminate material in areas that do not contribute significantly to the overall strength or function of the structure, resulting in an optimized design that maintains or enhances performance while reducing material waste. Although traditionally applied to materials like metals, topology optimization is increasingly being adapted for use with concrete, a vital material in the construction industry.

1.3 A general overview of 3D concrete printing.

3D concrete printing (3DCP), a form of additive manufacturing, allows for the layer-by-layer construction of complex concrete structures directly from digital models. This technology offers numerous advantages over traditional construction methods, such as the ability to fabricate intricate geometries, faster production times, and the potential for reducing material consumption. These capabilities make 3DCP particularly well suited for applications where precision and efficiency are critical.

When combined, topology optimization and 3D concrete printing can revolutionize the design and production of concrete structures. By incorporating topology optimization into the design phase of 3D printed concrete elements, it becomes possible to develop structures that use the least amount of material while still meeting all necessary strength and safety requirements. This integration is especially valuable in 3D concrete printing, where reducing material waste is not only a cost-saving strategy but also an environmentally sustainable approach. For instance, in the design of 3D concrete printed beams, topology optimization can help identify areas where concrete should be concentrated for strength and where it can be minimized without compromising the structural integrity. This approach leads to the creation of beams that are both lightweight and strong, reducing material costs and the environmental impact of construction.

1.4 Objective of this study

The main objective of this study is to explore the application of topology optimization for designing a material efficient concrete beam. The specific objectives are as follows:

1. Perform topology optimization of a concrete beam: By using Ansys Workbench, a concrete beam of dimension 500 mm x 100 mm x 20 mm is to be optimized by minimizing compliance and achieve a design that minimizes the material usages while keeping the structural integrity.
2. Develop a 3D printable concrete mix: A concrete mix is to be designed by trial and error method, which is suitable for 3D printing machine.
3. To perform tests for 3D printable concrete mix: The mix need to be extrudable, buildable and flowable. Hence, respective testes need to be performed.
4. Fabrication of optimized beam using 3D concrete printing: Utilizing the extrusion based technique and using a 3D concrete

printer , the topology optimized concrete beam of size 500 mm x 100 mm x 100 mm is to be printed adhering to the design specifications and enduring it is free from printing defects.

5. Fabricate beams of different infill: Employ a 3D concrete printer to construct beams with different infill ensuring the printed beam is free from printing defects.

6. To conduct a four-point flexural test: The printed beams need to be tested for load at which beam fails.

7. Analyse and compare the results: Assess the material efficiency and structural performance. In addition, check the feasibility of the topology optimized concrete in comparison to traditional design methods and beams with different infill patterns. The result also needs to highlight the advantages and potential challenges of integrating topology optimization with 3D concrete printing.

Chapter 2

2. Literature Review

2.1 General

Topology optimization (TO) be a computational design method that optimizes material layout for maximum performance under given loads. From its early inception (e.g. Michell's truss problems (M.C.E. 1904) (Ostoja-Starzewski 2001)) through modern methods e.g. SIMP – Solid Isotropic Material with Penalization (Tcherniak 2002) , Topology optimization has enabled lightweight, efficient structural forms (Zhu, Zhang, and Xia 2015).

The structural engineering community is increasingly focusing on sustainable technologies that reduce material usage and carbon emissions. Traditional concrete construction is resource-intensive and relies heavily on formwork, skilled labor, and sequential curing processes. In this context, 3D concrete printing (3DCP) has emerged as a disruptive method, offering automated, mold-free construction with complex geometries and significant material savings (Beghini (2013).

Parallel to these developments, topology optimization has matured as a powerful tool for structural design, aiming to find the most efficient material distribution within a given design space under specified loading and boundary conditions. The integration of topology optimization with 3DCP opens new avenues in designing optimized, structurally efficient, and environmentally sustainable building components.

2.2 Early Development in Topology Optimization

The mathematical foundation of topology optimization was laid by Bendsøe and Kikuchi (1988), who introduced the homogenization method for optimizing material layouts in continuum structures. This was followed by the SIMP (Solid Isotropic Material with Penalization) model, which provided a practical implementation of the optimization

problem using density variables. Researchers like Bruggi (2008) tackled challenges such as the stress singularity problem using modified interpolation schemes in the SIMP framework. Further improvements introduced compliance-based and stress-constrained formulations, with significant work by Bruggi and Duysinx (2012) in handling materials with unilateral behavior, such as concrete that behaves differently under tension and compression.

2.3 Software and code based Optimization

Yi, Cheng, and Xu (2016) proposed a topology optimization framework for heterogeneous periodic beam structures that effectively integrates commercial FEM software such as ANSYS and ABAQUS. Their approach uses the Asymptotic Homogenization (AH) method to derive effective stiffness properties of unit cells and employs gradient-based optimization with analytical sensitivity analysis. A key strength of their method is its ability to function as a "black-box" module within commercial solvers, leveraging their pre-processing and solver capabilities while adding custom optimization logic externally

Zuo and Xie (2015) developed a compact 100-line Python code that executes 3D topology optimization through the Abaqus Scripting Interface (ASI). The code adopts the Bi-directional Evolutionary Structural Optimization (BESO) method and interfaces with ABAQUS/CAE to handle FEA tasks, making it possible to process complex geometries imported from CAD software. Their work exemplifies the efficiency and transparency of integrating customized optimization algorithms into established commercial platforms. Aranda et al. (2020) presented Toptimiz3D, a standalone topology optimization platform that supports unstructured meshes in both 2D and 3D. While it is not tied to commercial software, it draws on open-source FEM libraries (e.g., MFEM) and uses Python and C++ for user interaction and solver implementation. Toptimiz3D implements the SIMP method, supports various solvers like MMA, OC, IPOPT, and includes post-

processing options compatible with Para View. Its key contribution is bridging academic flexibility and real-world mesh handling in a user-friendly format. Tyflopoulos and Steinert (2022) conducted a comparative study of SolidWorks, ANSYS Mechanical, and ABAQUS in the context of structural topology optimization. Using three benchmark geometries (bell crank, pillow bracket, and small bridge), they evaluated software performance in terms of optimization time, feature accessibility, and design output quality. The study found that while all three platforms support SIMP-based compliance minimization, they differ in pre-processing flexibility, solver speed, and support for manufacturing constraints. This evaluation highlights how different commercial tools serve different user needs depending on project scale and complexity. Liu and Tovar (2014) introduced a 169-line MATLAB code for 3D topology optimization, targeting educational and entry-level research users. Although not tied to commercial FEM software, the code integrates key features like finite element analysis, SIMP-based material interpolation, sensitivity filtering, and non-linear solvers like MMA and SQP. It provides an accessible platform for learning and prototyping, especially in academic settings where license access may be restricted. Jankovics et al. (2018) present an ANSYS®-integrated topology optimization framework specifically tailored for additive manufacturing (AM) constraints. The method is implemented using ANSYS Parametric Design Language (APDL), allowing full integration with ANSYS' finite element solver and GUI. Jankovics et al. (2018) demonstrate that the algorithm successfully converges to structures that eliminate the need for support material, thereby reducing material waste, post-processing time, and cost.

2.4 Application of Topology Optimization in Structural Design

Topology optimization has transitioned from academic formulations to real-world structural design problems. Jewett and Carstensen (2019) demonstrated that topology-optimized concrete beams could significantly reduce material volume while retaining structural capacity. Similarly, (Wang et al. 2025) validated optimized truss beams through experimental flexural testing and finite element modeling, achieving a 94% improvement in strength-to-weight ratio over traditional RC beams. Moreover, (Vantyghem et al. 2020) applied post-tensioning techniques to topology-optimized girders fabricated via 3DCP, marking one of the earliest integrations of reinforcement and optimization in large-scale printable elements. (Bruggi and Cinquini 2011) developed an optimization framework based on heat conduction equations to minimize thermal transmittance in building components, demonstrating how topology optimization can effectively mitigate thermal bridges and optimize the placement of insulation material. (Briseghella et al. 2013) illustrated the utility of topology optimization in the seismic retrofitting of bridges, where they optimized the thickness and shape of a bridge's superstructure. This allowed for a 40% reduction in weight, ensuring compliance with updated seismic codes without the need to reinforce the existing foundations. Hagishita and Ohsaki (2009) introduced the Growing Ground Structure Method (GGSM) for topology optimization, which allows for the iterative addition and removal of bars and nodes to achieve the optimal truss configuration. Avelino et al. (2018) applied density-based topology optimization to guide post-tensioned tendon layouts in flat-slab buildings under gravity loads, aiming to reduce compliance and optimize stiffness. (Tsavdaridis 2015) discussed how topology optimization can be used to create aesthetically and structurally efficient designs for complex structures, such as the Bionic Tower in Abu Dhabi.

2.5 Material Mix Design for 3D Concrete Printing

3D printable concrete (3DPC) has emerged as a transformative material in construction, enabling customized, automated, and efficient structural fabrication. A critical component in this innovation is the development of optimal mix designs that ensure printability, buildability, and mechanical performance. A comprehensive review by Hou et al. (2021) highlights the critical performance requirements of 3D printed concrete (3DPC), such as printability, rheology, and interlayer bonding, which are crucial for ensuring structural integrity and durability. This review synthesizes key findings from six recent studies, each contributing unique perspectives and methodologies to the field of 3DPC mix design. Khan (2020) provides a comprehensive review of mix types suitable for extrusion-based concrete 3D printing, identifying rheological properties like yield stress, plastic viscosity, and thixotropy as central to achieving pumpability and buildability. The study also addresses the importance of layer bonding and the effect of printing parameters such as time gap and nozzle size on structural integrity. (Ji et al. 2019) demonstrated the successful implementation of 3D printed ready-mixed concrete with coarse aggregates, showcasing practical applications in constructing large-scale infrastructure like power substations. Tay et al. (2022) explored the creation of functionally graded concrete through varying 3D printing parameters, achieving significant improvements in strength-to-weight ratios, thus illustrating the potential for tailored material performance in structural applications. Giridhar et al. (2023) proposed practical mix design methodologies using locally available materials for 3D concrete printing, emphasizing the importance of flow characteristics, buildability, and flexural strength enhancement. (Pham et al. (2023) emphasize a practical mix proportion design method based on coefficient ratios of water, sand, and fibers to the binder. The approach effectively balances extrudability and layer adhesion, crucial for maintaining geometric fidelity and mechanical stability during the printing process. Wang et al. (2022) investigate the inclusion of coarse aggregates in 3DPC, a notable shift from the fine mortar-dominated

mixtures typically used. The study demonstrates that controlled paste-to-aggregate ratios can enhance interlayer bonding, reduce mechanical anisotropy, and improve compressive strength. However, it also cautions that coarse aggregates can lead to pore irregularities during extrusion, impacting uniformity and strength. Xiong et al. (2024) explore a lightweight rubberized concrete using crumb rubber from waste tires as partial fine aggregate replacement. Despite a reduction in compressive strength with increased rubber content, the study highlights improved tensile strain, thermal insulation, and ductility, especially when reinforced with glass fibers. These characteristics make the material suitable for non-load-bearing walls in green building projects. In contrast, Sergis and Ouellet-Plamondon (2022) propose a multi-objective optimization framework using neural networks and genetic algorithms to minimize trial-and-error in mix design. Their system optimizes for flowability, buildability, and strength, demonstrating a significant reduction in the number of physical experiments needed by leveraging AI-driven predictions. Printability, buildability, and mechanical properties are the critical attributes of 3D printable concrete. Research has focused on enhancing rheological behavior through admixtures and fiber reinforcements. For instance, Lim et al. (2018) utilized micro-cable along with in-process steel cable reinforcement which showed enhancements in both flexural strength and ductility within geopolymer composites. Furthermore, studies have highlighted the bonding challenges between steel rebars and printed concrete layers, significantly affected by rheology, bar diameter, surface texture, and printing parameters. Nanomaterials such as nanosilica and fiber inclusions have also shown potential in reducing anisotropy and improving layer adhesion. Giridhar et al. (2023) developed a practical methodology for designing 3D printable concrete mixes using commonly available materials like cement, silica fume, fly ash, and limestone powder, along with steel and polypropylene fibers. The research underscores the need for practical testing tools, such as the flow table test, over complex rheometers for on-site applications.

2.6 Research Gap

Despite significant progress, several critical research gaps persist in the field:

- Bonding Performance: Current studies report inconsistencies in bond quality between printed concrete and embedded reinforcements, leading to unpredictable failure modes.
- Anisotropy: Most mechanical tests focus on ideal loading conditions. The influence of anisotropy in layer deposition on flexural and compressive strength remains under-characterized.
- Experimental Scaling: Most studies are limited to laboratory-scale specimens. Few works address full-scale or in-situ printed structural members, which are critical for practical implementation.
- Material-Specific Optimization: Most optimization methods assume isotropic or homogeneous material behavior, which is not representative of printed concrete with directional reinforcement or layer interfaces.
- Although studies assess properties such as buildability, extrudability, and interlayer bonding, there is no universally accepted standard or benchmark for evaluating these fresh-state characteristics. Most testing protocols are lab-specific or adapted from conventional concrete testing, which affects reproducibility and comparability across studies.
- While the incorporation of coarse aggregates reduces shrinkage, cost, and carbon footprint, it still presents significant challenges to printability and microstructural homogeneity. Research by Wang et al. (2022) shows that coarse aggregates cause irregular pore structures and anisotropic strength, but practical methods to mitigate these effects are underdeveloped.
- Many studies identify a direct trade-off between rheological performance (needed for printability) and hardened strength

(needed for structural integrity). However, a comprehensive framework to balance these conflicting properties through controlled mix design is still missing.

- Despite the potential environmental benefits, the long-term durability, structural reliability, and compatibility of sustainable materials like crumb rubber, recycled aggregates, or industrial by-products remain insufficiently studied—especially in the context of their interlayer bond strength and print precision.

- The interface between printed layers remains a weak zone, often responsible for lower tensile and flexural strength. Although some techniques (e.g., interlocking patterns, additives) are proposed, consistent strategies to enhance interlayer cohesion without affecting printability are still lacking.

- Very few studies evaluate the life-cycle costs, carbon footprint, or resource efficiency of proposed mix designs. Integrating sustainability metrics into mix design frameworks remains an underdeveloped but essential area for real-world implementation.

- Many topology optimization methods, including those implemented in ANSYS, ABAQUS, and custom solutions like Toptimiz3D and MATLAB-based scripts, suffer from mesh dependency. Research is needed to develop mesh-independent methods that can handle irregular geometries better, especially in the context of additive manufacturing where complex meshes are often involved.

- Existing software platforms still need enhanced capabilities to handle multi-material optimization in a seamless manner, considering both structural integrity and manufacturability.

- Despite the availability of powerful commercial software platforms (like SolidWorks, ANSYS, and ABAQUS), there is limited experimental validation to confirm the performance of optimized designs in real-world applications. Benchmarks with full-scale testing are often lacking, particularly in the case of additive manufacturing applications.

Chapter 3

METHODOLOGY

3.1 General overview
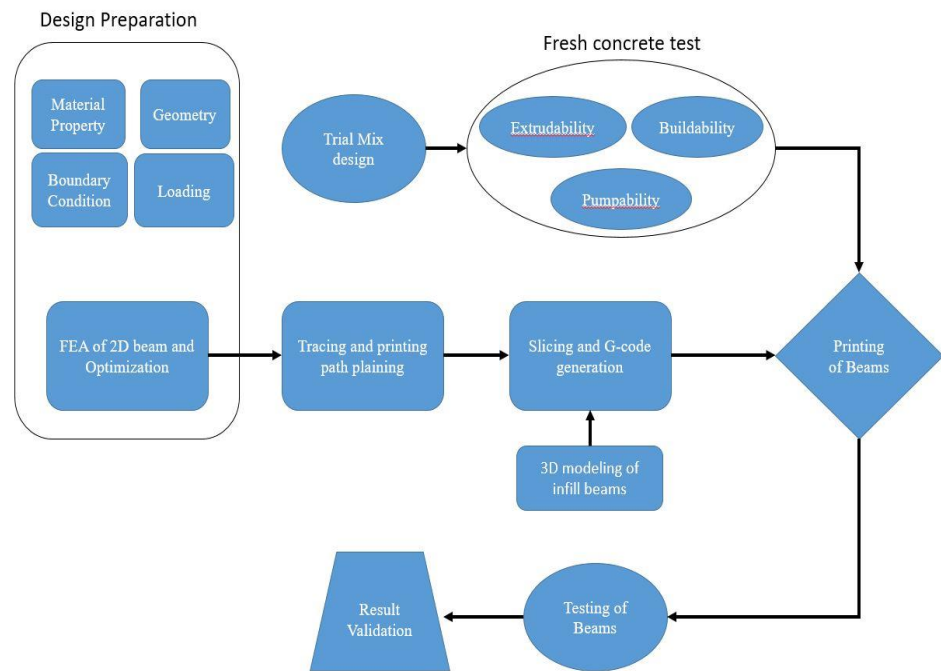
Figure 1 Flow chart of methodology

The methodology followed in this thesis work is shown in the form of flow diagram shown in figure 1.

The methodology for this research is organized into three major distinct phases.

1. Material mix design of 3D printable concrete (3DCP)
2. Develop and design of topology optimized beam
3. Fabrication and testing of beam.

The process begins with the design preparation phase, which includes conducting finite element analysis (FEA) on a 2D beam with dimensions of 500 mm x 100 mm x 20 mm. The beam is then optimized for minimum compliance, and the optimized 2D beam is converted into a 3D model using a tracing and path planning procedure. Additionally, two infill beams with N-shaped and S-shaped infills are modelled in SketchUp.

Once the beams are modelled, the optimized beam and the infill beams are sliced, and G-code is generated for the 3D printing process. A mix design for the concrete is developed using a trial-and-error method, focusing on key fresh concrete parameters such as buildability and extrudability. After finalizing the material mix and G-code, the design is fed into the 3D printer, and the concrete beams are printed using 3D concrete printing (3DCP) technology.

Subsequently, the printed beams undergo a four-point flexural test to determine the failure load and to analyse the failure patterns. The test results are then compared, and conclusions are drawn based on the performance of the beams

3.2 Trial and error method of mix design
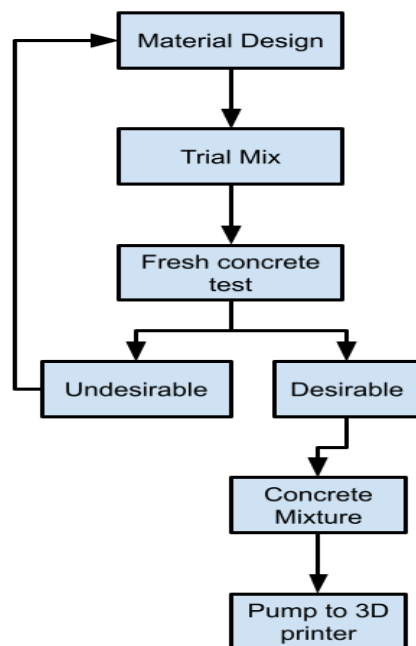
Figure 2 Flow diagram of developing printable concrete

The mix design of 3D printable concrete is a critical process that influences the printability, strength, and durability of the printed structure. This methodology details the approach followed for designing the mix through a trial-and-error method, considering key parameters such as buildability and extrudability.

The first step in designing a 3D printable concrete mix is selecting appropriate base materials. The choice of materials influences the performance of the concrete during the printing process. Based on the selected materials, a set of initial mix proportions is determined. This includes the amount of each material considering cement to aggregate ratio, cement to aggregate ratio and adjusting the proportion of superplasticizer and VMAs to achieve a workable mix.

3.3 Theory of topology optimization

The aim of topology optimization is to determine the most efficient material distribution within a structure to maximize or minimize a specific objective, such as global stiffness or natural frequency, while satisfying predefined constraints, such as mass reduction. In this study, the focus is on maximizing static stiffness, which can be interpreted as minimizing the structure's compliance. Compliance refers to the amount of work done on the structure by an applied load. A lower compliance indicates that less work is required from the load to deform the structure, meaning that less energy is absorbed, and the structure exhibits greater stiffness.

Mathematically,

$$\text{Compliance} = \int_v fu\,dV + \int_s tu\,dS + \sum_i^n F_i u_i$$

Where,

f = Distributed body force

F_i = Point load on i^{th} node

t = Traction force

u = Displacement field

u_i = ith displacement degree of freedom

S = Surface area of the continuum

V = Volume of the continuum

ANSYS uses gradient-based methods for topology optimization, where the design variables are continuous rather than discrete. These methods rely on a penalization technique to develop accurate material and void topologies. One of the most widely used penalization schemes is **SIMP** (Solid Isotropic Material with Penalization), which is discussed in the following section.

3.3.1 Solid Isotropic Material with Penalization (SIMP) method

The **SIMP** (Solid Isotropic Material with Penalization) method is a penalization approach commonly used in gradient-based topology optimization. It serves as the foundation for evolving a 0-1 topology.

In the SIMP method, each finite element, created through meshing in ANSYS, is assigned a pseudo-density value, denoted as x_j, where $0 \leq x_j \leq 1$. This pseudo-density modifies the stiffness properties of the material, enabling the optimization process.

$$x_j = \frac{\rho_j}{\rho_o}$$

Where.

ρ_j = Density of the jth element

ρ_o = Density of the base material

x_j = Pseudo-density of the jth element

16

The pseudo-density of each finite element acts as the design variable in the topology optimization process. The Pseudo-density of jth element depends on its Pseudo- density in a way that,

$$K_j = x_j^p K_o$$

Where,

K_o = Stiffness of the base material

$p > 1$ = Penalization power

When $x_j = 0$

$K_0 = 0$, meaning there is no material

When $x_j = 1$

$K_0 = 1$, meaning there is presence of material

In the SIMP method, the value of p is typically set greater than 1 to penalize intermediate densities. This ensures that the resulting design favors either solid or void material distributions, as intermediate densities would lead to reduced stiffness compared to the material volume. By increasing the value of p above 1, the optimization process discourages the use of intermediate densities, promoting a 0-1 material distribution in the final design.

In practical terms, when the volume constraint is active, choosing a sufficiently large value for p ensures that the optimization yields designs with minimal or no intermediate densities. Generally, a p value greater than 1 is required to achieve a 0-1 topology, which results in fully solid or void elements in the optimized design.

In ANSYS, the standard formulation for topology optimization involves minimizing structural stiffness or maximizing the system's fundamental frequency, all while adhering to a volume constraint. Another variant of the problem involves maximizing the natural frequency of the structure under dynamic loading, again subject to the same volume constraint.

The objective function in topology optimization is typically the compliance of the structure, which represents the amount of work done under applied loads. As the usable volume decreases, the stiffness of the structure also decreases, meaning that the volume constraint is inherently opposing the optimization objective of maximizing stiffness.

The Compliance of a descritized finite element can be written as,

$$c(x) = F^T u$$

The force vector being function of design variables x_j is written as,

$$K(x)u = F$$

Therefore, $c(x)$ can be written as,

$$c(x) = u^T K u = \sum_{j=1}^{n} u_j^T k_j(x_j) u_j$$

$$Subject\ to \sum_{j=1}^{n} x_j v_j \leq V_o$$

$0 < x_{min} \leq 1$ j = 1, 2, 3, …..n

A lower limit has been imposed on the design variables to prevent singularities in the stiffness matrix.

3.4 Optimality Criterion Approach

The discrete topology optimization problem involves a large set of design variables, denoted as N. Due to the complexity of the problem; it is common to apply iterative optimization techniques for its solution. In each iteration of the OC method, the design variables are updated using a heuristic approach.

The optimization problem is defined using the Lagrangian as follows.

$$L(x_j) = u^T K u + \alpha \left(\sum_{j=1}^{n} x_j v_j - V_o \right) + \lambda_1 (Ku - F)$$

$$+ \sum_{j=1}^{n} \lambda_2^j (x_{min} - x_j) + \sum_{j=1}^{n} \lambda_3^j (x_j - 1)$$

Where $\lambda_1, \lambda_2 \lambda_3$ and α are Lagrange multipliers for various constraints. The optimality condition is given by:

$$\frac{\partial L}{\partial x_j} = 0$$

Where j = 1,2,3,....,n

The Compliance is given by:

$$L = u^T K u$$

Differentiating equation with respect to the optimality condition we get

$$B_j = \frac{\dfrac{\partial C}{\partial x_j}}{\alpha v_j} = 1$$

The Compliance sensitivity can be given as

$$\frac{\partial C}{\partial x_j} = -p(x_j)^{p-1} u_j^T K_j u_j$$

Using these expressions, the design variables are revised as follows:

$$x_j^{new} = \begin{cases} max(x_{min} - m), if \ x_j B_j^\eta \leq (x_{min}, x_{min} - m) \\ x_j B_j^\eta, if \ max(x_{min} - m) < x_j B_j^\eta < min(1, x_j + m) \\ = min(1, x_j + m, if \ min(1, x_j + m) \leq x_j B_j^\eta) \end{cases}$$

In this context, m represents the move limit, which defines the maximum permissible change in x_j during a single iteration of the optimality criteria (OC) method. Additionally, η is a numerical damping coefficient, typically set to 1/2. The Lagrange multiplier associated with the volume constraint is determined in each optimality criteria iteration using a bisection algorithm. x_j denotes the density variable at each iteration step, while u_j represents the displacement field at each iteration, which is calculated from the equilibrium equations.

The optimization algorithm works as follow:

- Start with an initial design, such as a uniform material distribution.
- Using this density distribution, calculate the resulting displacements and strains through the finite element method.
- Compute the compliance of the design. If the improvement in compliance from the previous design is minimal, terminate the iterations. Otherwise, proceed with the next steps.
- Update the design variables using the method outlined in Equation 3.13. This step also involves an inner iteration loop to determine the value of the Lagrange multiplier α for the volume constraint
- Repeat the iteration process.

In this study, topology optimization capability of commercially available finite element analysis software called Ansys Workbench was used to optimize the beam

Figure 3 Flow diagram to show 3-step process of obtaining 3D optimized beam

3.5 Finite element analysis of 2D beam

The process of obtaining an optimized beam starts from generating an upstream feeder static structural analysis of 2D beam. After this analysis, the solution is linked with Structural Optimization System of Ansys.

Finite element analysis of 2D beam involves the following steps

- Assigning Material properties
- Creation of geometry of thin 2D beam
- Meshing of thin 2D beam
- Applying boundary condition
- Applying load
- Solving for required results i.e. stress, strain, deflection etc.
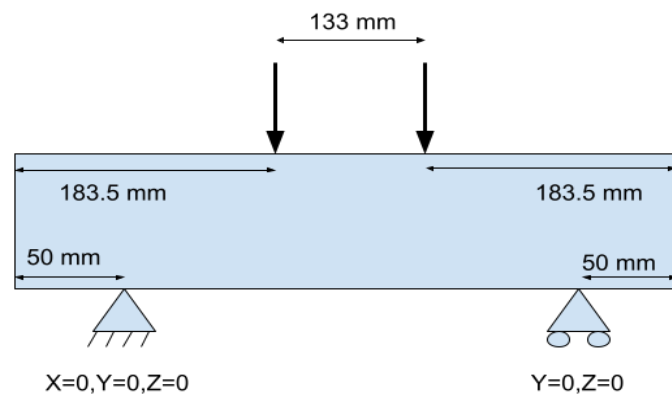
Figure 4 Support and loading condition

Material properties used in the simulation is as given in table 1.The thin 2D beam was sketched with dimensions 500 mm x 100 mm x 20 mm. The beam was meshed with 5 mm size hexagonal element. This size was chosen after mesh convergence analysis. The beam was supported as shown in the figure 2. A pin support at A was provided followed by a roller support at B. Both the supports were 50 mm from the nearest edge. The beam was loaded with two loads of 2500 N each at 183.5 mm distance from nearest edge.

Table 1. Material properties for FEA analysis

Material Properties used		Unit
Density (ρ)	1950	Kg/m^3
Modulus of Elasticity (Ec)	22360	MPa
Poisson Ratio (u)	0.2	-
Open shear transfer coefficient (Bo)	0.2	-
Close shear transfer coefficient (Bc)	0.8	-
Uniaxial cracking stress (Ft)	3.13	MPa
Uniaxial cracking stress (Fc)	20	MPa
Bulk Modulus	12422	MPa
Shear Modulus	9316.7	MPa

Chapter 4

OPTIMIZATION PROCESS

4.1 Topology Optimization of beam using Ansys Workbench.
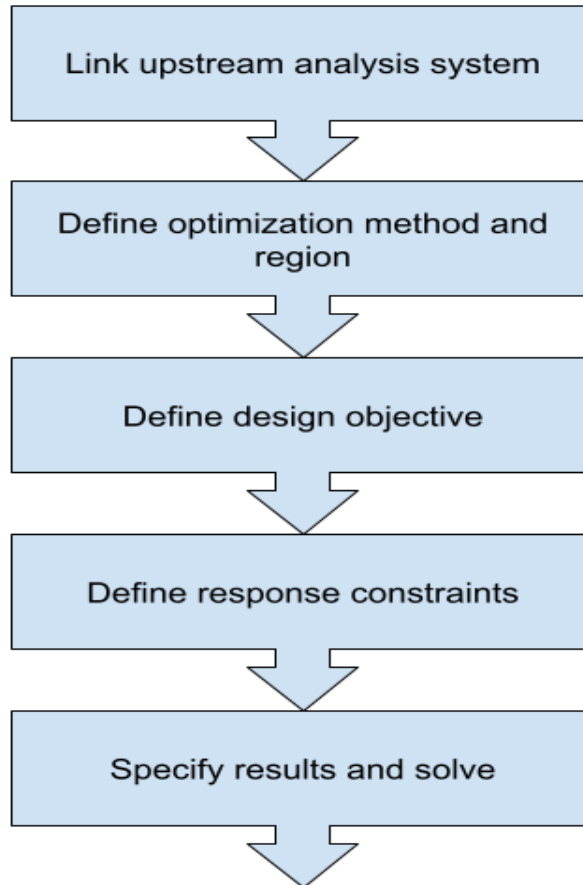
Figure 5 Flow diagram of optimization process

In this study, topology optimization capability of commercially available finite element analysis software called Ansys Workbench was used to get reference 2D optimized beam.

The first step is to link the static structural system of previously analysed 2D beam to the Structural Optimization system of the Ansys. This is done to share Engineering Data i.e. material properties, geometry and

model cells with the same cells as the upstream systems and the solution cell links to the setup cell of the Structural Optimization system as shown in figure 4.
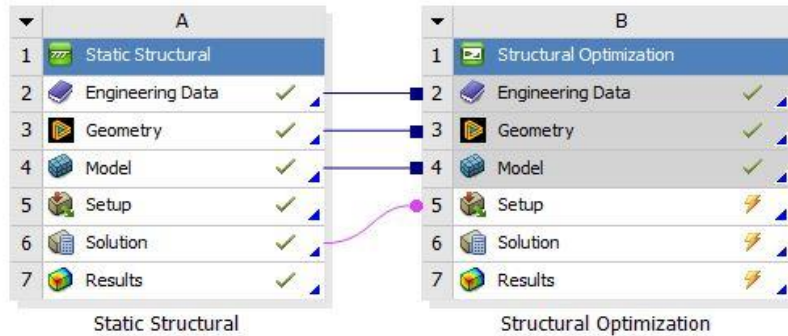

Figure 6 Linking of upstream analysis system to structural optimization system

In this study, density based topology optimization method was followed. All the boundary conditions were excluded from the optimization process so as to restrict the solver from removing materials from the supports and at the point of loading. The optimization was carried out for minimizing the compliance and maximizing the stiffness as an objective. Mass response constraint was studied and a 50 percent mass was restrained from removal. As a solution, beam geometry with topology density and topology elemental density results were obtained. The final model optimized beam geometry was obtained by changing the density threshold retention limit to 0.6. The optimized beam geometry as shown in figure 6 has uneven contour, which makes it, unfit for direct printing. Hence the optimized beam geometry was transferred to Spaceclaim module of Ansys Workbench for tracing out beam geometry and print path plaining.
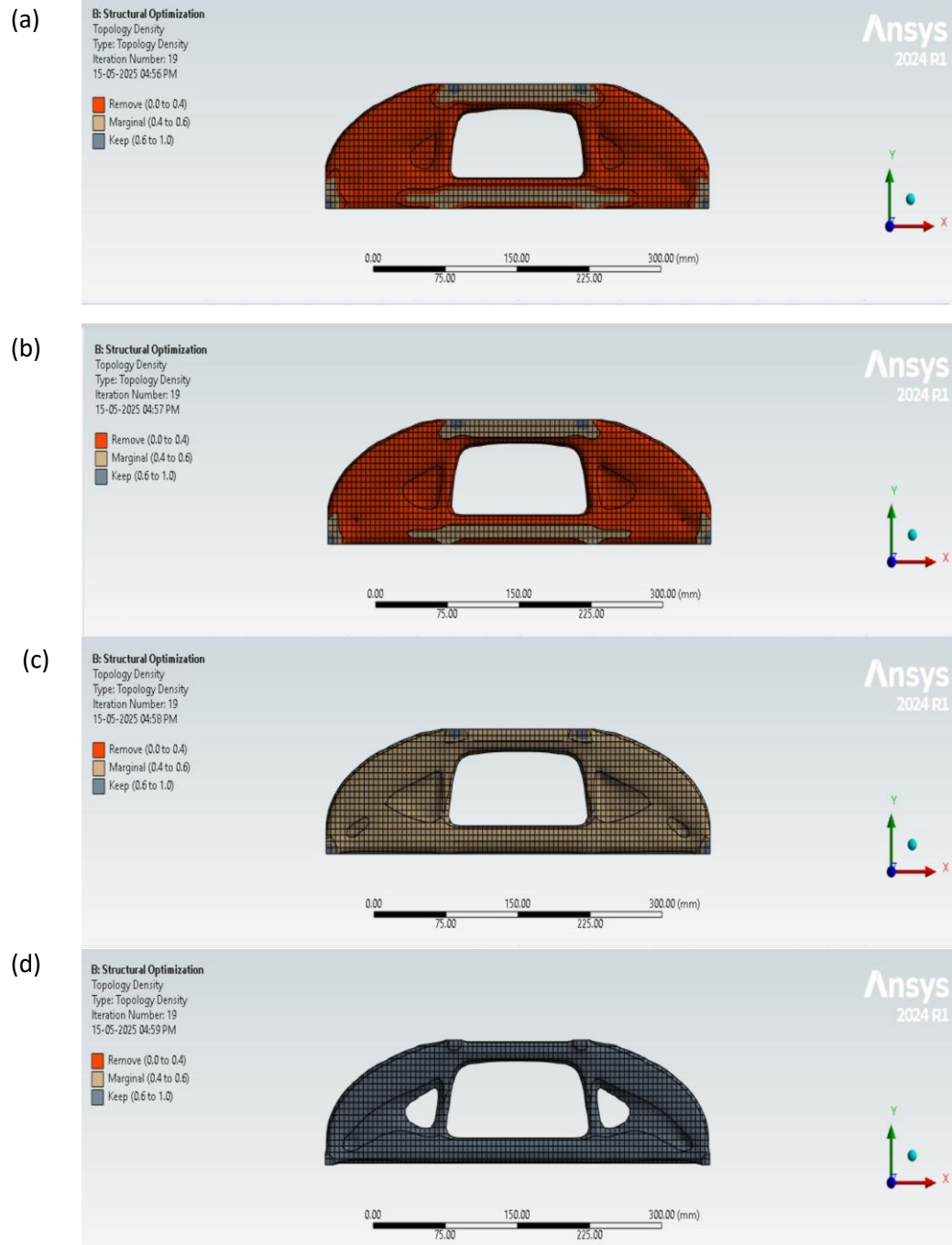
Figure 7 Model optimized beam at retention threshold value (a) 0.3, (b) 0.4, (c) 0.5, (d) 0.6
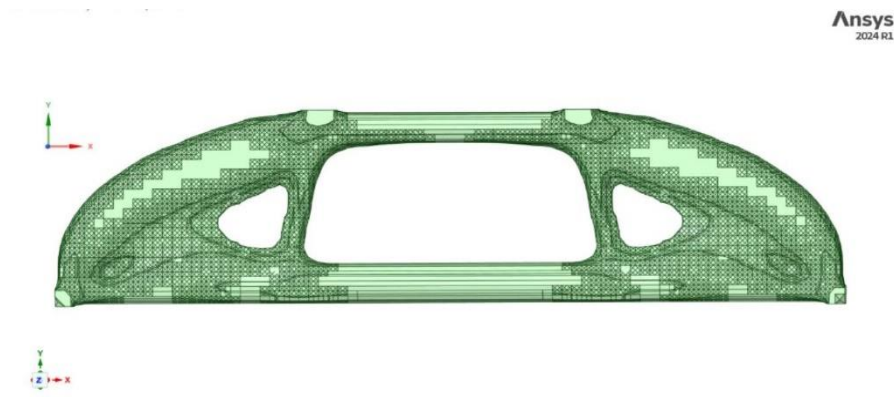
Figure 8 2D optimized beam as obtained after density based topology optimization

4.2 Print path plaining

Since the optimized beam has extrusion constraint, we have to find the best print path to print the beam. Printing with multiple start and end point leads to unwanted material extrusion on the layer and this leads to distortion of the geometry.

The model optimized beam was inspected and large mass locations were identified. It was then traced using straight lines and few curved lines to cover those areas as shown in figure 9.
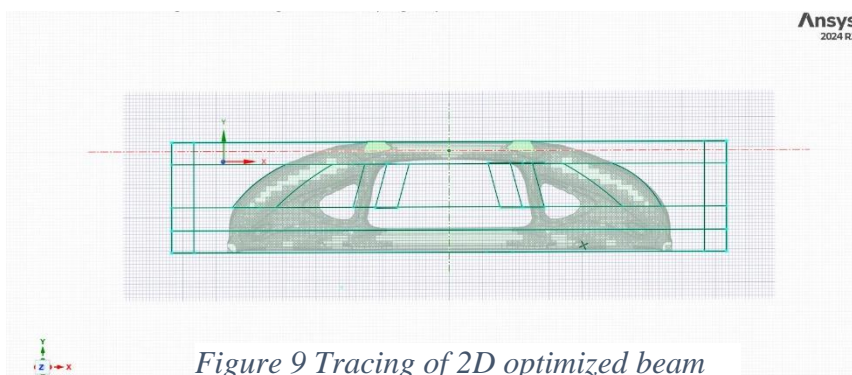
Figure 9 Tracing of 2D optimized beam

Along those areas the print path was identified so as to obtain single start and end points for layer extrusion as shown in figure 10. The beam so extruded so that in has a length of 500 mm and

a height of 100 mm to satisfy IS 516 part 1 four point flexure test specimen dimensions.
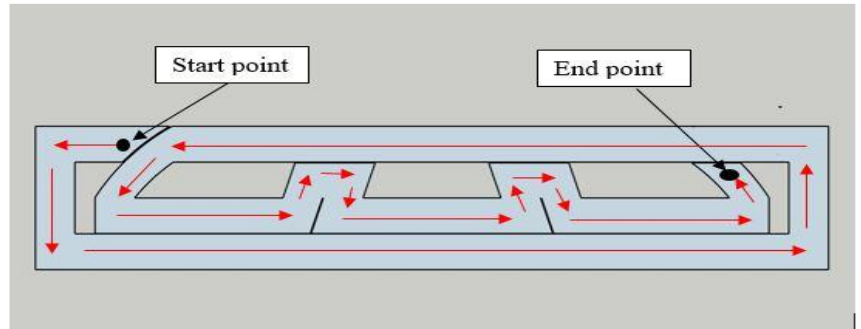
Figure 10 Layer print path

Final optimized 3D beam of dimension 500 mm x 100 mm x 100 mm was obtained after extruding the traced layer by 100 mm in z-direction as shown in figure 11.

Figure 11 Final optimized 3D beam

Chapter 5
MATERIAL MIX DESIGN

5.1 Overview

One of the objectives of the study was to develop concrete mixes suitable for 3D printing using simple tools, which would be practical for on-site applications. The study focused on formulating plain cement concrete using locally available materials, aiming to meet the requirements for 3D concrete printing (3DCP), such as extrudability, buildability, and stability after extrusion. Flow diagram for the same is as shown in figure 2.

5.2 Material used

5.2.1 Cement

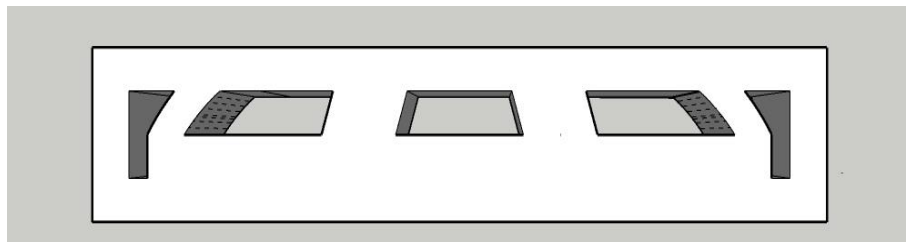OPC of grade 43 complying to Indian Standard code 12269:1987 is used in this study without any partial replacement by supplementary cementitious materials. The specific gravity of 3.15 was used for all the mix design trials. The particle size of the cement lies between 31 microns to 7.5 microns. The final and initial setting times were 255 minutes and 110 minutes. The normal consistency was measured to be 32%.

5.2.2 Aggregate

Sand serves as the primary fine aggregate in 3D printable concrete and plays a critical role in determining the mix's flowability, surface finish, and mechanical strength. Unlike conventional concrete, which may utilize a range of particle sizes, 3D printable concrete typically requires well-graded, fine sand with a controlled particle size distribution—often below 2 mm—to ensure smooth extrusion through the nozzle and prevent clogging. The shape and texture of sand particles also influence the rheological behavior of the mix; rounded particles tend to enhance workability, while angular particles can improve inter-layer bonding but may reduce flowability. Natural river sand, manufactured sand (M-

sand), and crushed stone sand are commonly used, provided they are free from impurities such as clay, silt, or organic matter. In some cases, sieving is performed to achieve the desired fineness modulus and consistency across batches. The optimization of sand characteristics is essential not only for ensuring pumpability and print quality but also for maintaining the structural performance of the printed elements. Therefore, careful selection and quality control of sand are vital for the success of 3D concrete printing applications. In this study, natural river sand was used with gradation as shown in figure 12. The maximum size of sand used is 1.18 mm.
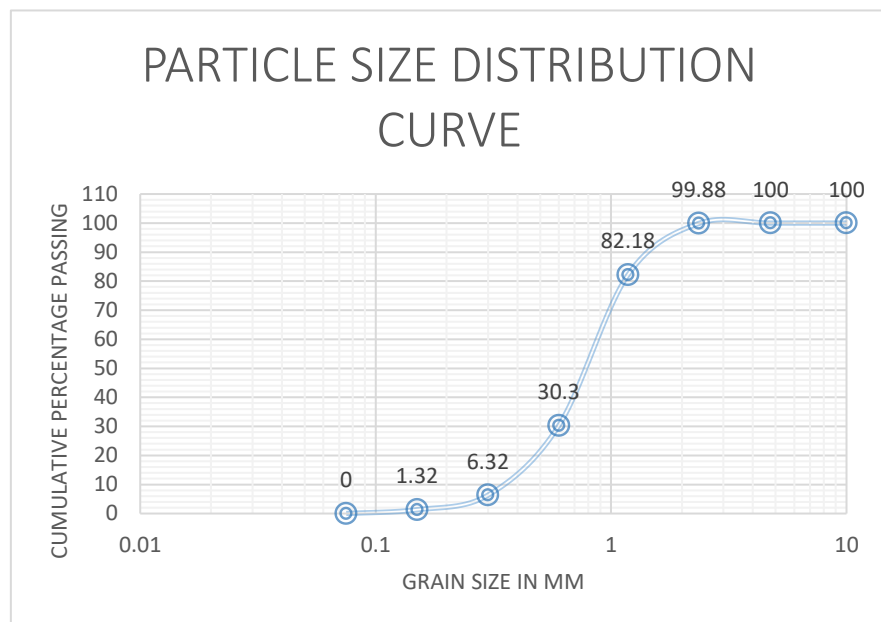
Figure 12 Particle size distribution curve for fine aggregate

5.2.3 Water

Water is one of the fundamental material, which is very much essential for hydration of cement. Its amount in the form of water to cement ration greatly influence the strength of the 3D printable concrete. In case of 3D printable concrete, the mix has to be so designed that the concrete is has adequate flow property for pumping and extrusion while maintaining its shape during printing and prevent layer collapse. Increasing the amount of water will lead to low strength in 3D printable concrete and reducing

in excess will lead to non pumpable concrete. Also as per IS 456: 2000 the pH of the water shall be more than equal to six. The water should be free from oils, acids, alkalis, organic materials or salts. Portable water is generally considered suitable. In 3D printable concrete, precise control of water content is critical, as minor variations can lead to significant changes in rheological behavior, affecting both extrusion consistency and layer adhesion. Thus, both the quality and quantity of water must be rigorously managed to ensure optimal performance of 3D printed structures.

5.2.4 Clay

Clay, when incorporated into 3D printable concrete, functions as a mineral additive that influences both the rheological properties and the sustainability profile of the mix. Its fine particle size and high surface area contribute to enhanced cohesion, which is particularly beneficial in maintaining the shape and stability of extruded layers. Certain types of clay, such as kaolinite or bentonite, are known for their thixotropic behavior, enabling the concrete to behave like a fluid under shear during extrusion and regain stiffness once the shear is removed. However, the quantity and type of clay must be carefully controlled, as excessive use may lead to increased water demand and reduced strength. Nano clay was used in this study.

5.2.5 VMA

Viscosity Modifying Agent (VMA) is essentially needed to enhance the printability and stability of 3D printable concrete. VMA affects the rheological property of 3D printable concrete by increasing its viscosity without significantly affecting flowability. They contribute to the thixotropic behavior of 3D printable concrete, which means the concrete flows under the shear stress of pumping but regains viscosity once extruded. Common VMAs are cellulose ethers, welan gum and other ploysccharide based compounds.

5.2.6 Superplasticizer

The superplasticizers are high range water reducing admixtures, which has a very crucial role of reducing the water requirement of 3D printable concrete. Since 3D printable concrete requires high flowability for pumping, adding excess water for the same is not advisable, as it will severely affect the strength of 3D printable concrete. In this study polycarboxylate ether based superplasticizer was used.

5.3 Trial Mix

Trial mix was so formulated that the concrete maintained the proper flowability, buildability, and workability during the printing process while achieving the desired structural strength and durability once hardened.

Key Characteristics ensured while finalizing the mix was as follow:

- It was ensured that the final mix had sufficient viscosity to ensure it can flow easily through the nozzle but also maintain its shape once deposited.
- The trial mix was workable enough to allow for smooth extrusion, but it should set quickly enough to support subsequent layers without collapsing.
- The concrete mix should be able to support the weight of subsequent layers without deforming or sagging.
- The mix had appropriate curing properties to ensure that it hardens at a controlled rate and doesn't crack under the weight of new layers.

In this study, 3D printable concrete mix was finalized after making modifications in reference mix proportion on the basis of fresh cement concrete tests i.e. pumpability, buildability, flowability and extrudability.

Table 2: Trial mix proportions

Group	Name	Cement (kg)	Sand (kg)	Nano clay	SP (kg)	Water (kg)	VMA (kg)	Remarks
Group 1	3DCPM1	750	1080	8.75	0.6	376	9.75	True Slump- not printable
	3DCPM2	750	1080	8.75	0.6	376	6.375	True Slump- not printable
	3DCPM3	750	1080	8.75	0.6	376	4.85	140cm- not prinatble
	3DCPM4	750	1080	8.75	0.6	376	3.9	15cm flow- not printable
	3DCPM5	750	1080	8.75	0.6	376	2.925	17cm flow – Due to VMA stickiness
	3DCPM6	750	1080	8.75	0.6	376	1.95	Good mix with little stickiness (approx. 20 cm)
	3DCPM7	750	1080	8.75	0.6	376	0.975	Good mix, Extrudable and buildable (approx. 21 cm)
Group 2	3DCPM8	750	1080	8.75	0.6	376	0.975	Good mix (approx. 21 cm)
	3DCPM9	750	1080	8.75	1.2	376	0.975	Good mix with increased setting time (approx. slump flow 22 cm)
	3DCPM10	750	1080	8.75	2.4	376	0.975	Good mix with increased setting time (approx. slump flow 25 cm)
	3DCPM11	750	1080	8.75	4.8	376	0.975	Good mix, extrudable, (approx. slump flow 25 cm)
	3DCPM12	750	1080	8.75	9.6	376	0.975	Good mix, extrudable, not buildable (approx. slump flow 28 cm)
	3DCPM13	750	1080	8.75	11.25	376	0.975	Self settleable property, not buildable
	3DCPM14	750	1080	8.75	15	376	0.975	Self-flow property, not extrudable and not buildable

Figure 14 Print with trial mix 3DCPM8   *Figure 14 Print with trial mix 3DCPM12*

The trial was done in two groups. Group 1 and Group 2. At first, the reference mix was tested and found out that the slump obtained was true slump. In group 1 by keeping all the other parameters constant and reducing the VMA, a slump of 21 cm was achieved and in group 2 the VMA was kept constant and the SP was increased. From testing all the trial mix proportions, it was concluded that the mix 3DCPM7 was best among all. It had good extrudability and buildability both. It can be observed from figure 14 that the printed single layer is continuous throughout the length without breakage.

Chapter 6

FABRICATION AND EXPERIMENTAL TESTING OF BEAMS
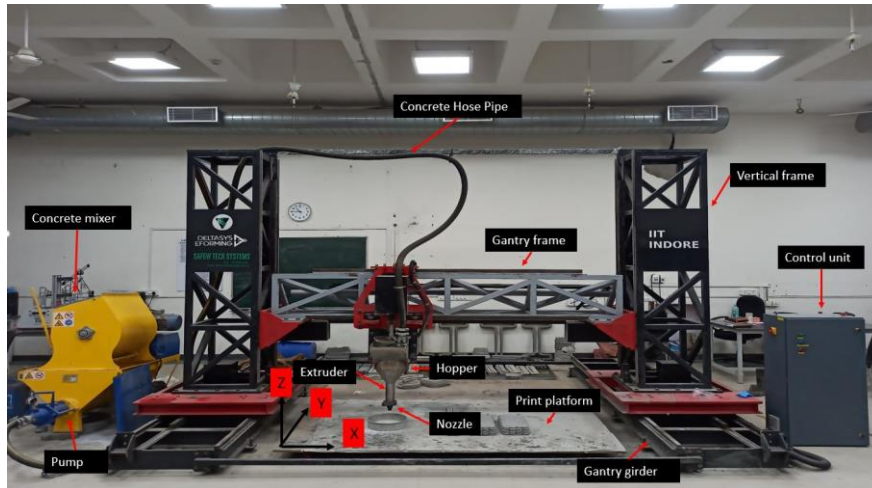
6.1 Gantry based 3D printer

Figure 15 Gantry based 3D printer

In this study large scale gantry based 3D concrete printer was used. A **gantry-based 3D concrete printer** uses a gantry system (a movable frame) to precisely control the deposition of concrete layers to create large-scale structures. This type of printer is designed for the construction industry and is capable of printing complex, custom shapes with concrete materials. It consists of several parts, each playing a crucial role in the operation and functionality of the 3D printer.

6.1.1 Key Parts of a Gantry-Based 3D Printer:

6.1.1.1 Gantry Frame:

This is the main framework of the printer, which supports all other components. The gantry frame is the primary structure of the printer that supports and enables movement of the extruder in three dimensions (X, Y, Z axes). It is typically made from rigid materials such as steel, aluminum, or carbon fiber for durability and stability. The X and Y-axes are guided by horizontal rails, allowing movement across the printing

area. The Z-axis is controlled by vertical rails, which move the print head up and down. The frame has cross beams to ensure stability, especially when dealing with large prints.

6.1.1.2 Print Head / Extruder:

The print head or extruder is responsible for depositing the concrete material. It is equipped with a nozzle through which the material flows and is printed layer by layer. The extruder pushes the concrete mix out through the nozzle, forming the desired shape. Extruder consists of nozzle which controls the size and thickness of the extruded concrete layers and agitator which agitators to prevent clogging and ensure smooth extrusion. Various types of nozzle is as shown in the figure 16.

Figure 16 Nozzle types

6.1.1.3 Material Delivery System:

This system supplies concrete material to the extruder. It includes the hopper, pump, and hoses that carry the concrete from the storage to the extruder. Hopper is container that holds the concrete mix (or mortar). Pump is used to transfer the concrete from the concrete mixer to the hopper from where it goes to extruder nozzle under consistent pressure.

6.1.1.4 Print Bed:

The print bed is the surface where the 3D concrete printer deposits material to construct the printed structure. It is usually made from concrete or a durable surface to handle the weight and size of the printed structure. The gantry based 3D printer used in the study had 2 m x 2 m print bed as shown in the figure 17.
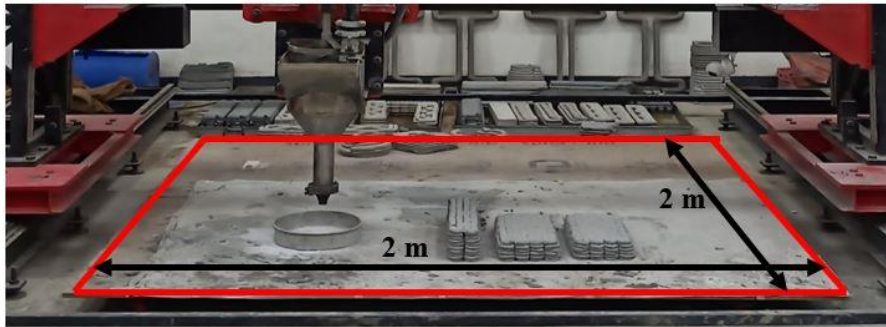

Figure 17 Print bed of the gantry based 3D concrete printer

6.1.1.5 Movement System (Motors and Actuators):

The movement system controls the movement of the gantry along the X, Y, and Z axes. It consists of Stepper Motors, Linear Rails and Bearings, and Servos or Linear Actuators. Stepper Motors are motors are responsible for precise movement along the X, Y, and Z axes. Linear rails guide the movement of the gantry frame and ensure smooth, accurate positioning. Bearings reduce friction and improve the efficiency of motion. Actuators precisely control the vertical and horizontal movement of the print head.

6.1.1.6 Control System / Control Unit:

The control unit is the brain of the printer. It processes the input from the operator and sends commands to the motors, extruder, and other parts of the printer to carry out the printing process. It manages the movement of the gantry and the print head. It controls the flow of concrete from the extruder based on the G-code.
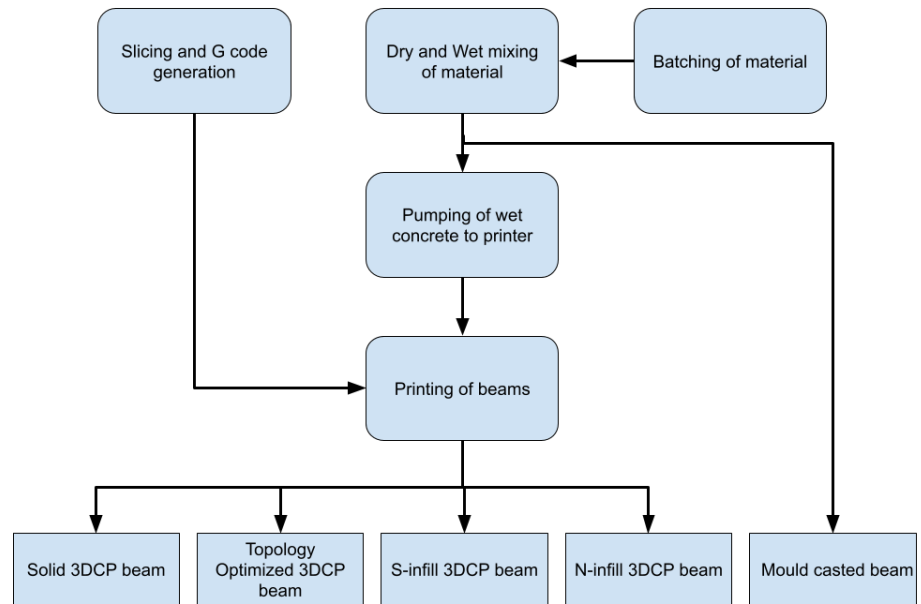
Figure 18 Flow diagram of printing process

Five types of beam geometry were designed in SketchUp software as shown in figure 18.
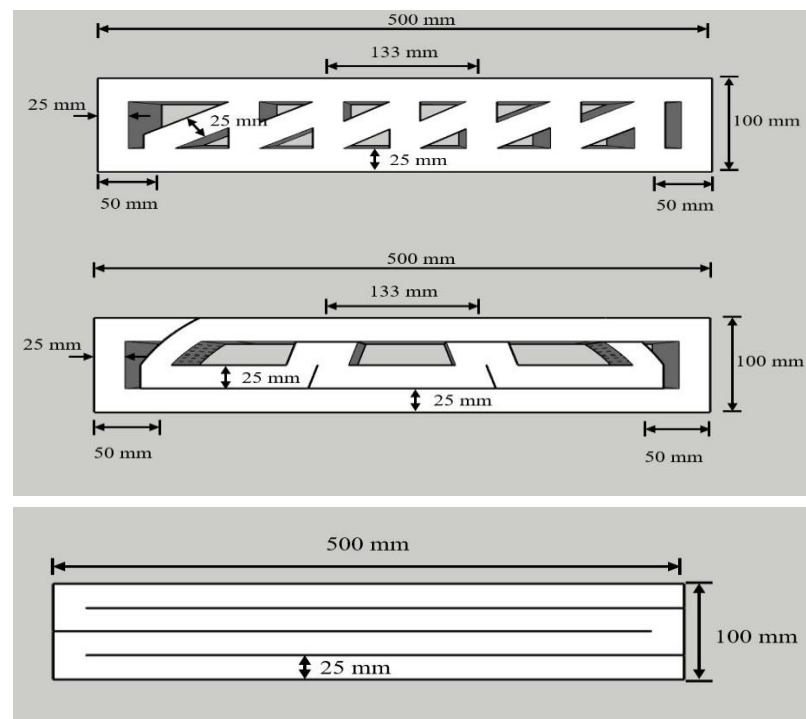

Figure 19 N-infill, optimized and solid 3DCP beams

6.2 Slicing and G code generation

Slicing is a critical step in 3D printing, where the 3D model of an object is divided into thin horizontal layers or slices. Each slice represents one layer of material to be printed, and the slicer software generates the corresponding print paths for the printer's nozzle to follow. Slicing determines the layer height, print speed, and path layout to ensure the beam is printed with structural integrity, efficiency, and minimal material waste.

In this study, Simplify3D software was used to slice four types of beams i.e. Printed solid beam, Optimized beam, S infill beam and N infill beam as shown in figure

The input parameters to slice the beams were as shown in the table 3.

Table 3: Input parameters for slicing and printing

Layer height	15 mm
Print speed	3000 mm/min
Nozzle dia	25 mm
Fill Density	0
Material flow rate	100-120 rpm

For the 3D printing of the concrete beam with dimensions of 500 mm x 100 mm x 100 mm, the following print parameters were selected to optimize the for slicing and printing process. The layer height was set to 15 mm, which is relatively thick and designed for fast production, while still ensuring adequate layer bonding. A print speed of 3000 mm/min was chosen to expedite the printing process, allowing for efficient material deposition without compromising the structure's integrity. The nozzle diameter was 25 mm, which is large enough to accommodate the required material flow for a concrete beam of this size, helping to reduce printing time while maintaining precision in material placement. The fill density was set to 0%. The material flow rate was controlled between 100–120 rpm, which regulates the extrusion speed of the concrete,

ensuring a consistent and controlled deposition of material for optimal layer bonding and structural stability. These settings are tailored to achieve a balance between print efficiency and the structural requirements of the beam. The sliced image of optimized beam is shown in figure 20.
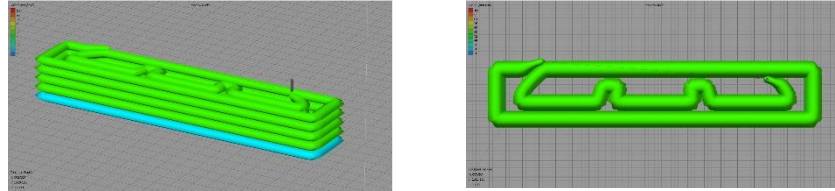

Figure 20 Sliced optimized beam geometry

After slicing, movement instruction for 3D concrete printer in the form of Gcode is generated for each beam geometry.

6.3 Material batching, mixing and printing

The materials were weighed in proportion of design mix 3DCPM8 as discussed in material design chapter. First all the dry components i.e. Ordinary Portland cement, natural sand, nano clay and VMA were batched in concrete mixer and dry mixed for about 5 minutes. Then half of the water was added and mixed for another 2 minutes. Super plasticized SP was dispersed in the remaining water and mixed for about 5 minutes at 360 rpm. The concrete was then pumped via pump hose to printer hopper to carryout the printing process of the beams.

Figure 21 Printing of S-infill 3DCP beam

Table 4: Specimens printed

Sl. No.	Name	Beam samples
1.	Solid 3DCP beam	
2.	Topology Optimized 3DCP beam	
3.	S-infill 3DCP beam	
4.	N-infill 3DCP beam	
5.	Mould casted beam	

Apart form the printed beams, the material was filled in the mould to obtain conventional casted beam of size 500 mm x 100 mm x 100 mm.

6.4 Defects in printing

6.4.1 Layer Misalignment or Shifting

Layer misalignment is another critical defect encountered during the printing of concrete beams, and it refers to the displacement or offset of one printed layer relative to the previous one. This misalignment results in visible gaps, uneven surfaces, or a structural discontinuity that can

severely compromise the strength, stability, and aesthetic quality of the printed beam.

In the case of the printed concrete beams, layer misalignment manifested as horizontal shifts between adjacent layers, particularly in areas where the printhead underwent sudden directional changes or when the printer experienced intermittent movement issues. Another contributing factor to layer misalignment was the material flow inconsistencies. The concrete mixture used in the printing process had a relatively high viscosity, and if the material did not flow smoothly from the nozzle, it could cause fluctuations in the extrusion rate. These fluctuations led to uneven material deposition, which in turn resulted in misaligned layers as the extruded material did not uniformly adhere to the surface of the previous layer.

To mitigate layer misalignment, several measures were taken. First, the printer calibration was rigorously checked and adjusted to ensure that the printhead movements were accurate and consistent. This involved verifying the stepper motors**,** guide rails, and alignment of the print bed to eliminate any mechanical inaccuracies. Additionally, the printing

Figure 22 Layer misalignment in beam

speed was optimized to reduce the risk of sudden movements that could lead to misalignment.

6.4.2 Initial extrusion delay

This defect happens when the nozzle fails to deliver a continuous flow of material at the start of the printing process, resulting in a gap or void in the printed beam at the beginning of the layer.

Figure 23 Initial extrusion delay defect

The common causes that was identified was improper nozzle priming and inconsistent material viscosity. Some other causes were improper calibration of extrusion system, partial blockage of nozzle or within the extrusion system. Missing material resulted in poor adhesion between subsequent layers leading to strength loss. It also give an unpleasant aesthetic appearance. This defect was over come by properly priming of nozzle at the beginning of the printing process. The material was properly mixed to obtain consistent viscosity.

6.4.3 Delamination

One of the significant defects encountered during the printing of the topology-optimized concrete beams was delamination, which refers to the failure of the bond between consecutive printed layers. Delamination occurs when the material of one layer does not adequately adhere to the previous layer, leading to the separation of the layers after or during the curing process. This defect is particularly critical in 3D concrete printing because it compromises the structural integrity and load-bearing capacity of the printed object.

Figure 24 Delamination of layer

During the printing process of the beams, delamination manifested in the form of visible gaps or weak zones at the interface between layers. These gaps were observed primarily in areas where the extrusion rate was not consistent, leading to insufficient material deposition or improper bonding. To mitigate delamination, it was necessary to adjust several printing parameters. Lowering the print speed and ensuring a more consistent extrusion flow helped create a smoother transition between layers.

6.4.4 Surface Imperfections

Surface imperfections are another common defect encountered during the printing of concrete beams, and they refer to any irregularities or inconsistencies on the outer surface of the printed structure. These imperfections can manifest as rough textures, visible lines, under-extrusion, or uneven finishing. In the context of 3D concrete printing, surface imperfections are not only aesthetically undesirable but can also affect the structural integrity and durability of the printed beam, as the surface plays a crucial role in load distribution and long-term performance. During the printing of the beams, surface imperfections were observed primarily in the form of uneven layering, where slight inconsistencies in the extrusion rate or material deposition led to visible ridges or grooves along the surface of the printed object. These imperfections were more prominent in areas where the print speed was either too fast or too slow, resulting in inconsistent material deposition. For example, when the printhead moved too quickly, there was a

tendency for the material to be under-extruded in certain regions, leaving gaps or an uneven surface finish. Conversely, when the printhead moved

too slowly, it could cause over-extrusion, leading to an accumulation of excess material and a rough, bumpy surface texture.
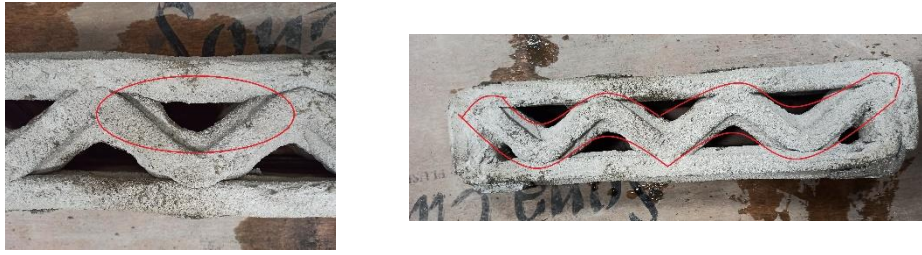

Figure 25 Surface imperfection due to under extrusion

To address surface imperfections, several strategies were employed during the printing process. Optimizing print speed and ensuring a consistent extrusion rate were crucial in maintaining an even deposition of material, which helped to avoid both under-extrusion and over-extrusion. Improved material mix design was also a key factor in minimizing surface defects. By adjusting the water-to-cement ratio and incorporating appropriate additives, the flowability of the material was enhanced, allowing for smoother deposition and better layer adhesion.

6.4.5 Blockages or Jamming in the Nozzle

During the printing of the topology-optimized concrete beams, nozzle jamming was one of the significant defects encountered, causing frequent interruptions in the printing process and resulting in uneven material deposition. Nozzle jamming refers to the obstruction or

blockage of the extruder nozzle, which prevents the smooth flow of material, halting the extrusion process or leading to under-extrusion in

Figure 26 Material deposition and jamming of nozzle

certain areas. the specific case of the concrete beams, nozzle jamming was observed in several stages of the printing process, primarily when there was a mismatch between the material viscosity and the extrusion settings. It was also observed that the nozzle jamming is more frequent in smaller diameter nozzle that larger diameter nozzle. Another factor that contributed to nozzle jamming was premature curing of the material. To mitigate the issue of nozzle jamming, several strategies were employed. First, the nozzle diameter was adjusted to match the properties of the concrete mix. The mix design chosen in this study worked well with 25 mm diameter nozzle and lead to lower frequency of nozzle jamming.

6.4.6 Inconsistent Layer Height

Inconsistent layer height emerged as a significant defect during the printing of the topology-optimized concrete beams, resulting in uneven surfaces and compromised structural integrity. Layer height, which refers to the vertical distance between each deposited layer of material, plays a crucial role in determining the resolution and overall quality of the printed object. For a beam, especially one subjected to structural loads, uniformity in layer height is essential for ensuring proper bonding between layers, effective load distribution, and maintaining dimensional accuracy. During the printing process, variations in layer height caused irregularities in the surface finish and affected the interlayer adhesion, leading to potential weak zones in the final structure.

Figure 27 Inconsistent layer height

To mitigate inconsistent layer height, several measures were implemented during the printing process. Material mix design was optimized to improve the flowability and consistency of the concrete,

ensuring that the mix would extrude uniformly and form even layers without variations in thickness. Additionally, print speed and layer height were optimized based on the material's properties and the required structural strength. By adjusting the layer height to a slightly larger value (such as 15 mm), the print was able to proceed more efficiently, but this required careful control over the material's flow and extrusion rate to ensure that the print quality remained consistent.

6.5 Experimental testing

6.5.1 Compression Strength Test

Compression testing was performed to determine the compressive strength of the designed 3D printable concrete mix. To perform the test, cubes of size 50 mm x 50 mm x 50 mm were cut from the slab as shown in figure 29. The load was applied in three different planes of the cube.

Table 5: Compression test results

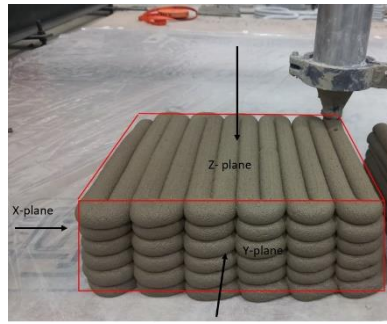| Sample loaded on	Sample 1	Sample 2	Sample 3	Average	Comp. Strength	STD Dev
Z plane (S1)	58	52	55	55	22	2.44949
Y plane (S2)	62	60	58	60	24	1.632993
X plane (S3)	50	51	55	52	20.8	2.160247

Figure 28 Casting of slab

Figure 29 Marking of slab for cube cutting

Figure 31 Compression testing of cube

Figure 30 Cutting of slab

6.5.2 Four-Point Flexural Test of Topology Optimized and Comparison Beams

The aim of this experiment was to evaluate the flexural performance of a topology optimized 3D printed concrete beam using a four-point bending test. The optimized beam's behavior was compared with that of a conventionally mould casted beam, and four additional 3D printed beams namely solid 3DCP beam, S-infill 3DCP beam and N-infill 3DCP beam, respectively. The goal was to investigate whether topology optimization provides enhanced structural behavior, particularly in terms of load to weight ratio.

All beams were made using the same concrete mix and were cured under identical conditions. The 3D printed beams were produced layer-by-layer using a gantry-based extrusion system with consistent layer height and print speed. The four-point bending test was conducted according to IS 516 2021 part 1 standards using a universal testing machine. The support span was 400 and load was applied with two rollers at one third of supporting span. Load at a rate of 1.8 KN/min was applied. Observations were made for load at failure and deflection.

Figure 32 Crack formation and ultimate failure of topology optimized 3DCP beam

Table 6: Failure load of various beams

Sr. No.	Name	Failure Load
1.	Solid 3DCP beam	6.09
2.	Topology Optimized 3DCP beam	5.78
3.	S-infill 3DCP beam	4.31
4.	N-infill 3DCP beam	3.6
5.	Mould casted beam	6.304

Chapter 7

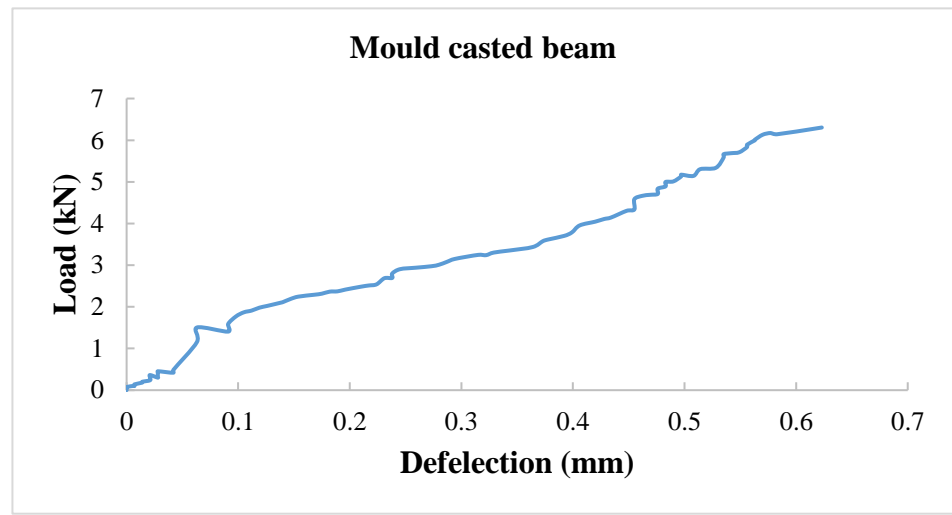# RESULTS AND DISCUSSION

7.1 Load vs deflection

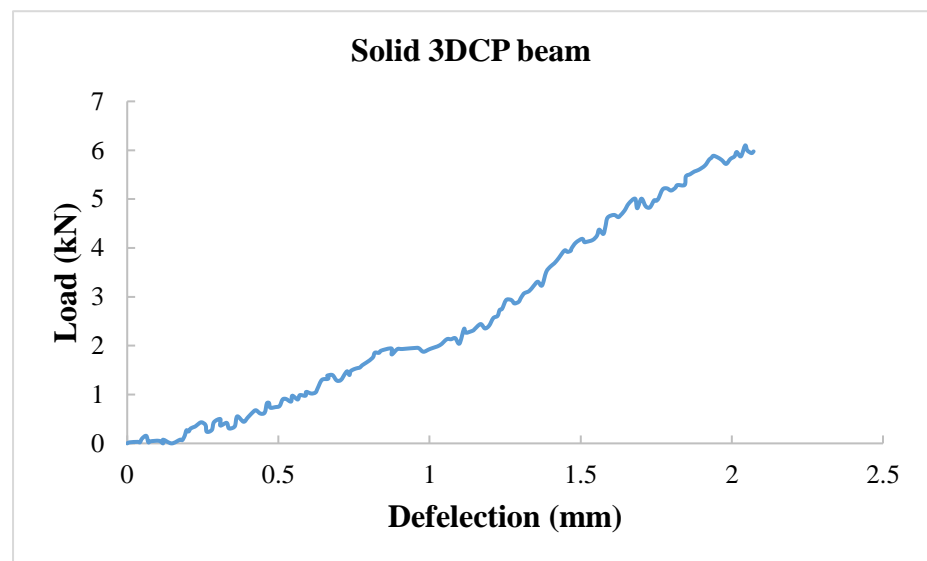*Figure 33 Load vs deflection curve of Mould casted beam*

Figure 34 Load vs deflection curve of Solid 3DCP beam
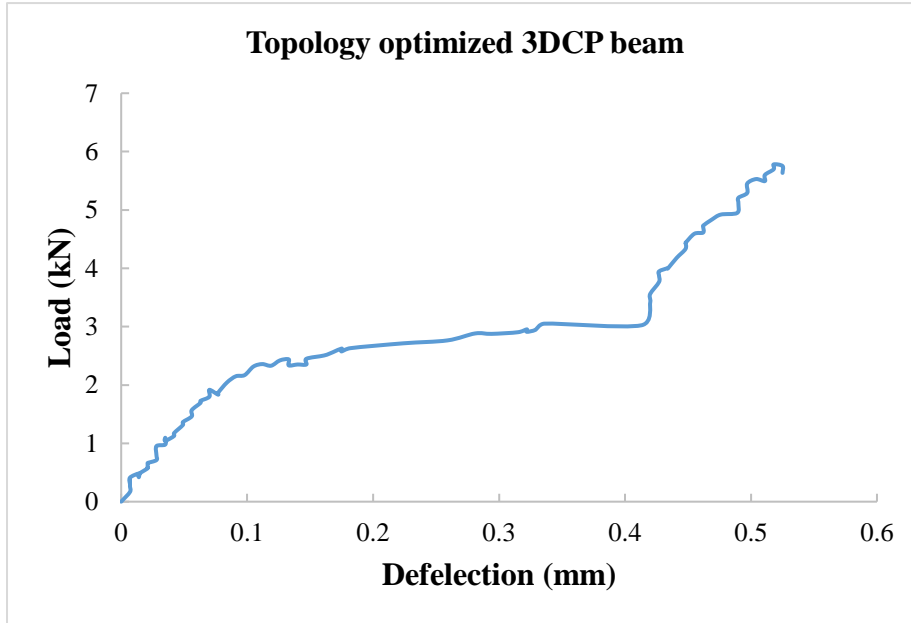
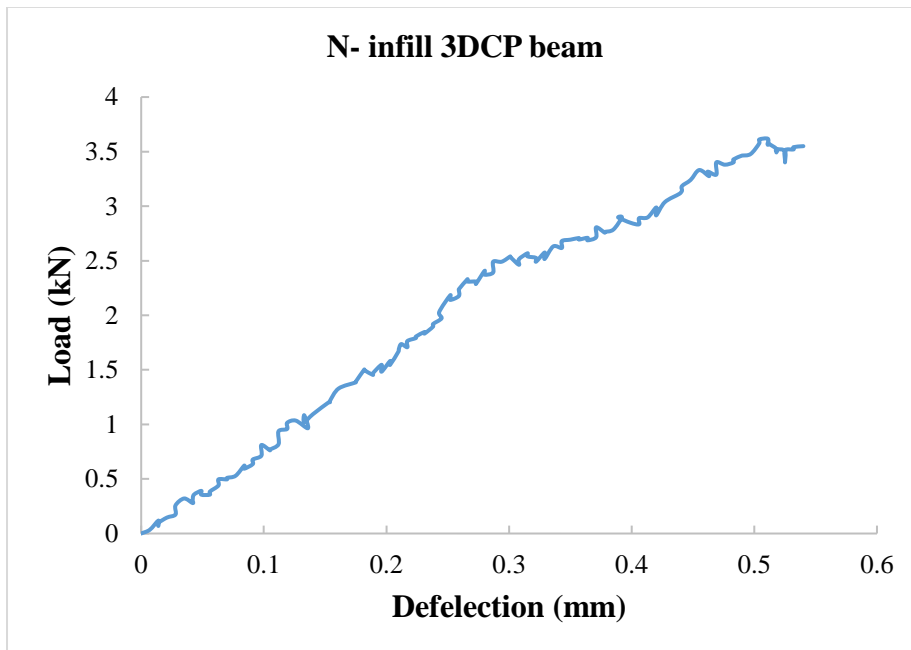*Figure 35 Load vs deflection curve for topology optimized 3DCP beam*

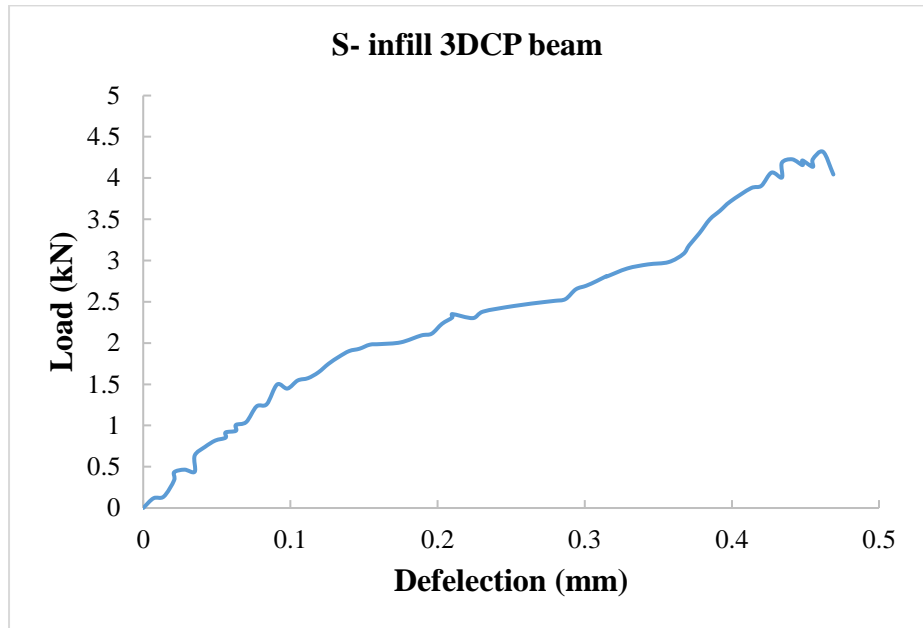*Figure 36 Load vs deflection curve of N-infill 3DCP beam*

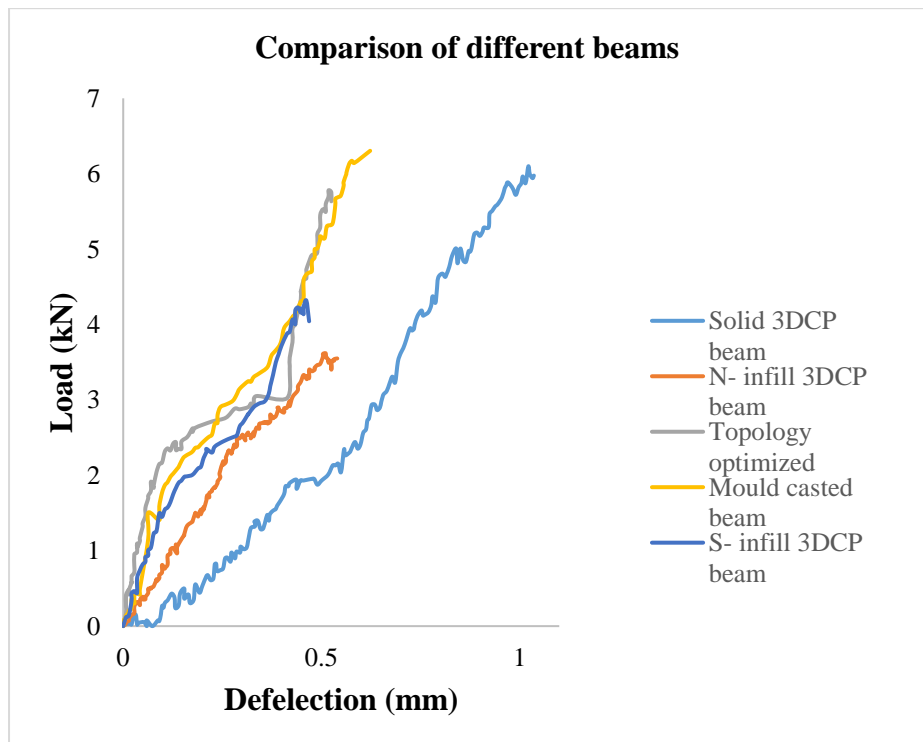*Figure 37 Load vs deflection curve of S-infill 3DCP beam*

Figure 38 Combined load vs deflection curve

The failure load and deflection behaviour of the different types of 3DCP beams were as follows:

- Solid 3DCP Beam: This beam exhibited a failure load of 6.09 kN with a deflection of 1.036 mm. Among all the tested beams, it had the highest deflection, indicating superior strain hardening properties.
- N-infill 3DCP Beam: The failure load of this beam was 3.55 kN, with a deflection of 0.54 mm. Despite having the lowest failure load among all the beams, it demonstrated better strain hardening behavior than the S-infill and mould casted beams.
- S-infill 3DCP Beam: With a failure load of 4.318 kN and a deflection of 0.469 mm, the S-infill beam had the lowest deflection compared to all the other beams.
- Mould Casted Beam: This beam displayed the highest failure load of 6.304 kN with a deflection of 0.623 mm.
- Topology Optimized 3DCP Beam: The failure load of the topology optimized beam was 5.78 kN, with a deflection of 0.525 mm. The load-deflection curve of this beam showed a linear behaviour up to a 0.1 mm deflection. Beyond 0.1 mm, the load increased more gradually until 0.4 mm, after which the load increased sharply, reaching 5.78 kN.

This comparison reveals that the Solid 3DCP beam exhibits the best strain hardening property, while the N-infill 3DCP beam demonstrates improved strain hardening despite its lower failure load.
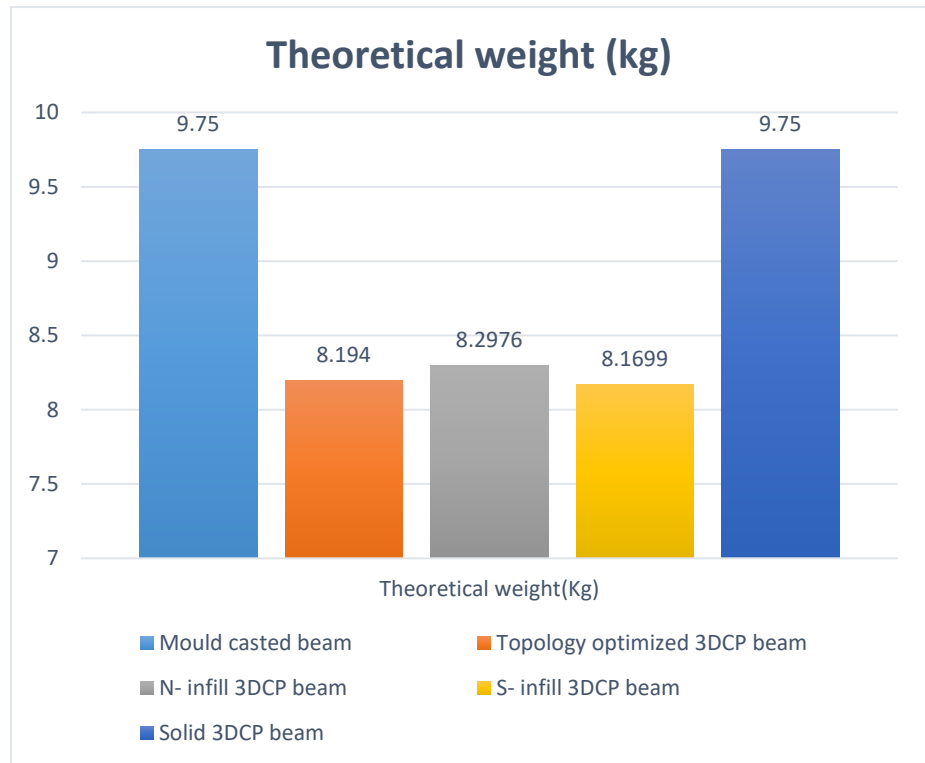
Figure 39 Bar chart of theoretical weight comparison
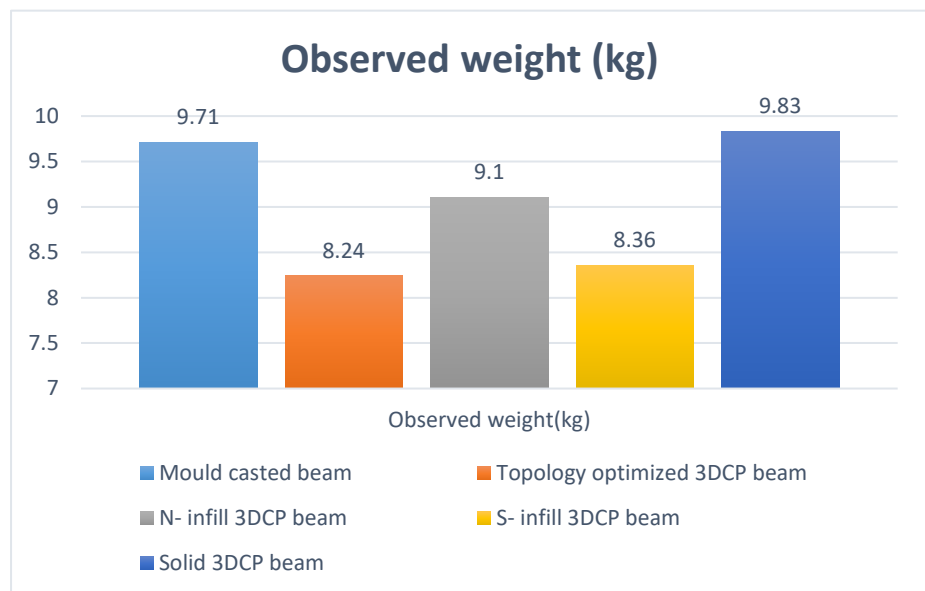
Figure 40 Bar chart of observed weight comparison
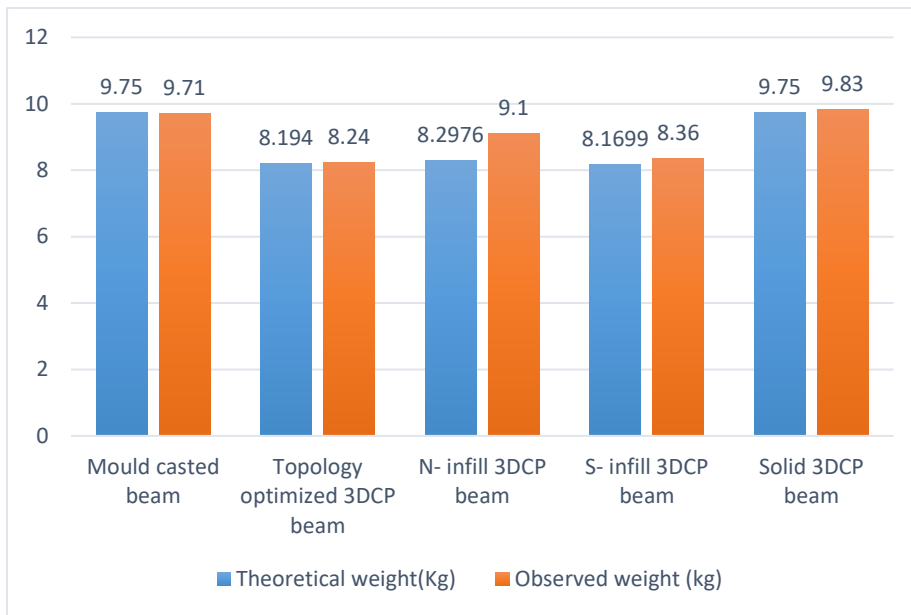
Figure 41 Comparison of theoretical and observed weight
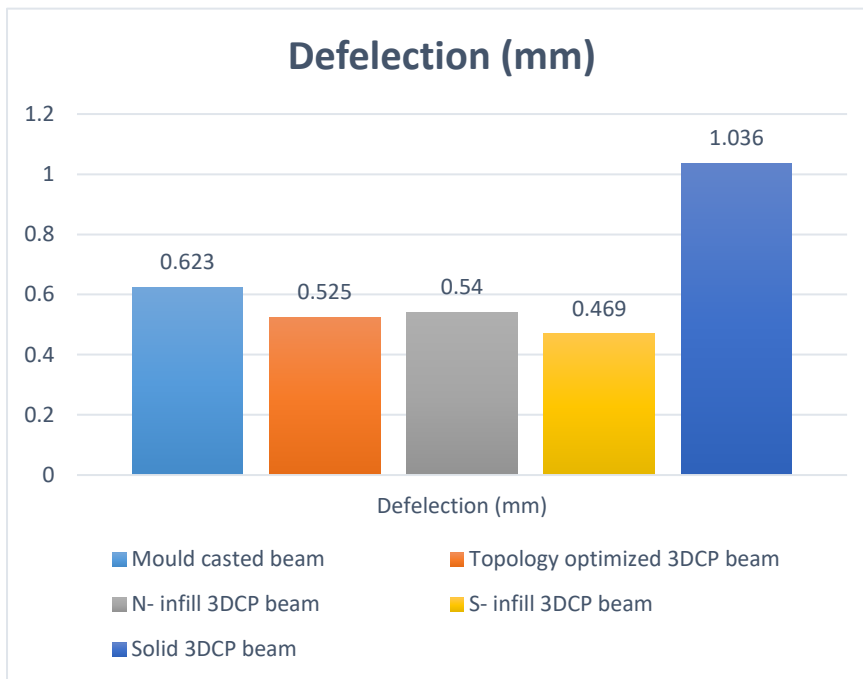
Figure 42 Bar chart of deflection comparison
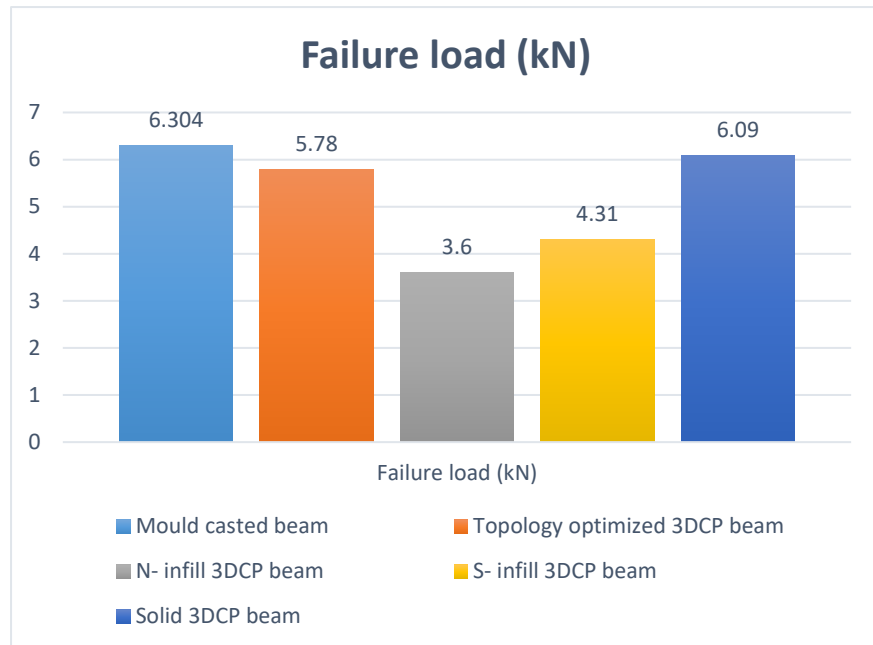
Figure 43 Bar chart of failure load comparison

Figure 44 Bar chart of strength to weight ratio comparison

7.2 Weight comparison

Theoretically, the Mould casted and Solid 3DCP beams are of equal weight, at 9.75 kg, making them the heaviest among all the beams. The S-infill 3DCP beam, on the other hand, weighs 8.1699 kg, making it the

lightest. Theoretically, the Topology optimized 3DCP beam weighs 8.194 kg, ranking as the second lightest beam, as shown in Figure 39. As seen in Figure 41, all the beams, except the mould casted beam, are heavier than their theoretical weight. The maximum difference between the theoretical and actual observed weight was found in the N-infill beam, with a variation of 9.6%. This discrepancy can be attributed to difficulties in achieving precise extrusion during the 3D printing process, which was affected by material heterogeneity. Variations in material properties during printing led to inconsistencies in extrusion, causing the beams to be heavier than initially expected.

7.3 Failure Load comparison

The load-carrying capacity of all the beams, in descending order, is as follows:

Mould casted beam > Solid 3DCP beam > Topology optimized 3DCP beam > S-infill 3DCP beam > N-infill 3DCP beam.

The maximum load-carrying capacity in the four-point flexure test was observed in the Mould casted beam, which withstood a load of 6.304 kN. The minimum failure load, on the other hand, was recorded in the N-infill 3DCP beam, at 3.6 kN. The Topology optimized 3DCP beam failed at a load of 5.78 kN, which is approximately 8.31% less than the Mould casted beam.

7.4 Strength to weight ratio

In this study, strength is defined by the maximum load that the beam can withstand up to failure. The lowest strength to weight ratio was observed in N-infill 3DCP beam and the highest strength-to-weight ratio was achieved by the Topology optimized 3DCP beam, with a ratio of 0.701. The Topology optimized 3DCP beam exhibits a 8.04% higher strength-to-weight ratio compared to the conventional Mould casted beam.

7.5 Conclusion

It is observed that after attaining ultimate failure load, all the beams suddenly failed which shows the brittleness of the material.

It can be observed from figure 39 that solid 3DCP beam has two times deflection than mould casted beam having almost similar failure load.

S-infill 3DCP beam had lowest deflection and N-infill 3DCP has lowest failure load among all beams.

The main objective of this study was to design and develop an optimized beam. This objective was achieved by developing Topology optimized 3DCP beam having 8.04 percent better strength to weight ratio than conventional Mould casted beam.

It can be concluded that topology optimized beam can perform better for same amount of material used as compared to conventional mould casted beams.

This work demonstrates that commercial software like Ansys Workbench can be used to design and develop optimized beam.

This study demonstrates that 3D printable concrete can be be developed using basic construction materials.

Chapter 8
FUTURE SCOPE

- Future research could focus on exploring the use of alternative 3D printing technologies, such as multi-material printing, to enhance the mechanical properties and functionality of the optimized beam.
- Additionally, investigating the effects of varying printing parameters and material compositions on the performance of topology-optimized concrete beams could provide insights into further improving the strength-to-weight ratio.
- The integration of reinforcement in the design, coupled with advanced printing techniques, could also be examined to explore the synergy between optimization algorithms and traditional reinforcement strategies.
- Moreover, scaling up the design for practical applications, such as in large-scale structural components or in combination with sustainable materials, could be a valuable direction for future studies.
- Shape optimization can also be explored for developing aesthetically pleasing structural members.

REFRENCES

1. Aranda, Ernesto, José Carlos Bellido, and Alberto Donoso. 2020. "Toptimiz3D: A Topology Optimization Software Using Unstructured Meshes." *Advances in Engineering Software* 148:102875. doi:10.1016/J.ADVENGSOFT.2020.102875.

2. Avelino, Ricardo M., David Shook, Alessandro Beghini, Eric Long, and Mark Sarkisian. n.d. "Efficient Flat-Slab Post-Tensioning Layouts Guided by Topology Optimization."

3. Beghini (2013). 2013."Building Science through Topology Optimization - ProQuest." https://www.proquest.com/openview/5bef60078114dba3ab292cab 35dc8317/1?cbl=18750&pq-origsite=gscholar.

4. Bendsøe, Martin Philip, and Noboru Kikuchi. 1988. "Generating Optimal Topologies in Structural Design Using a Homogenization Method." *Computer Methods in Applied Mechanics and Engineering* 71(2):197–224. doi:10.1016/0045-7825(88)90086-2.

5. Briseghella, B., L. Fenu, C. Lan, E. Mazzarolo, and T. Zordan. 2013. "Application of Topological Optimization to Bridge Design." *Journal of Bridge Engineering* 18(8):790–800. doi:10.1061/(ASCE)BE.1943-5592.0000416/ASSET/B344F184-D189-4280-A11F-B92FCECB09D3/ASSETS/IMAGES/LARGE/FIGURE18.JPG.

6. Bruggi, Matteo. 2008. "On an Alternative Approach to Stress Constraints Relaxation in Topology Optimization." *Structural and Multidisciplinary Optimization* 36(2):125–41. doi:10.1007/S00158-007-0203-6/METRICS.

7. Bruggi, Matteo, and Carlo Cinquini. 2011. "Topology Optimization for Thermal Insulation: An Application to Building Engineering." *Engineering Optimization* 43(11):1223–42. doi:10.1080/0305215X.2010.550284;PAGE:STRING:ARTICLE/CHAPTE R.

8. Bruggi, Matteo, and Pierre Duysinx. 2012. "Topology Optimization for Minimum Weight with Compliance and Stress Constraints." *Structural and Multidisciplinary Optimization* 46(3):369–84. doi:10.1007/S00158-012-0759-7/FIGURES/17.

9. Deaton, Joshua D., and Ramana V. Grandhi. 2014. "A Survey of Structural and Multidisciplinary Continuum Topology Optimization: Post 2000." *Structural and Multidisciplinary Optimization* 49(1):1–38. doi:10.1007/S00158-013-0956-Z/FIGURES/14.

10. Giridhar, Greeshma, Prabhat Ranjan Prem, and Shankar Kumar. 2023. "Development of Concrete Mixes for 3D Printing Using Simple Tools and Techniques." *Sadhana - Academy Proceedings in Engineering Sciences* 48(1):1–13. doi:10.1007/S12046-022-02069-W/FIGURES/12.

11. Global Status Report for Buildings and Construction 2024/2025 | UNEP - UN Environment Programme. n.d.

https://www.unep.org/resources/report/global-status-report-buildings-and-construction-20242025.

12. Global Status Report | GlobalABC. n.d. https://globalabc.org/global-status-report.

13. (Green Rating for Integrated Habitat Assesment). n.d. https://www.grihaindia.org/manuals.

14. Hagishita, T., and M. Ohsaki. 2009. "Topology Optimization of Trusses by Growing Ground Structure Method." *Structural and Multidisciplinary Optimization* 37(4):377–93. doi:10.1007/S00158-008-0237-4/METRICS.

15. Hou, Shaodan, Zhenhua Duan, Jianzhuang Xiao, and Jun Ye. 2021. "A Review of 3D Printed Concrete: Performance Requirements, Testing Measurements and Mix Design." *Construction and Building Materials* 273:121745. doi:10.1016/J.CONBUILDMAT.2020.121745.

16. IGBC | IGBC Green New Buildings Rating System. n.d. https://igbc.in/igbcgreennewbuildings/.

17. Jankovics, Davin, Hossein Gohari, Mohsen Tayefeh, and Ahmad Barari. 2018. "Developing Topology Optimization with Additive Manufacturing Constraints in ANSYS®." 51(11):1359–64. doi:10.1016/J.IFACOL.2018.08.340.

18. Jewett, Jackson L., and Josephine V. Carstensen. 2019. "Topology-Optimized Design, Construction and Experimental Evaluation of Concrete Beams." *Automation in Construction* 102:59–67. doi:10.1016/J.AUTCON.2019.02.001.

19. Ji, Guangchao, Tao Ding, Jianzhuang Xiao, Shupeng Du, Jun Li, and Zhenhua Duan. 2019. "A 3D Printed Ready-Mixed Concrete Power Distribution Substation: Materials and Construction Technology." *Materials 2019, Vol. 12, Page 1540* 12(9):1540. doi:10.3390/MA12091540.

20. Khan, M. A. 2020. "Mix Suitable for Concrete 3D Printing: A Review." *Materials Today: Proceedings* 32:831–37. doi:10.1016/J.MATPR.2020.03.825.

21. Lim, Jian Hui, Biranchi Panda, and Quang Cuong Pham. 2018. "Improving Flexural Characteristics of 3D Printed Geopolymer Composites with In-Process Steel Cable Reinforcement." *Construction and Building Materials* 178:32–41. doi:10.1016/J.CONBUILDMAT.2018.05.010.

22. Liu, Kai, and Andrés Tovar. 2014. "An Efficient 3D Topology Optimization Code Written in Matlab." *Structural and Multidisciplinary Optimization* 50(6):1175–96. doi:10.1007/S00158-014-1107-X/FIGURES/12.

23. M.C.E., A. G. M. Michell. 1904. "LVIII. The Limits of Economy of Material in Frame-Structures." *The London, Edinburgh, and Dublin Philosophical Magazine and Journal of Science* 8(47):589–97. doi:10.1080/14786440409463229.

24. Ostoja-Starzewski, M. 2001. "Michell Trusses in the Presence of Microscale Material Randomness: Limitation of Optimality." *Proceedings of the Royal Society A: Mathematical, Physical and*

Engineering Sciences 457(2012):1787–97.
doi:10.1098/RSPA.2001.0777;PAGE:STRING:ARTICLE/CHAPTER.

25. Pham, Loan Thi, Thu Nguyen, Thanh Trinh, Anh Nguyen, Quang Do, Bien Bui, and Jianzhuang Xiao. 2023. "Development of 3D Printers for Concrete Structures: Mix Proportion Design Approach and Laboratory Testing." *Smart and Sustainable Built Environment* 12(5):1056–73. doi:10.1108/SASBE-07-2022-0137.

26. Sergis, Vasileios, and Claudiane M. Ouellet-Plamondon. 2022. "Automating Mix Design for 3D Concrete Printing Using Optimization Methods." *Digital Discovery* 1(5):645–57. doi:10.1039/D2DD00040G.

27. Tay, Yi Wei Daniel, Jian Hui Lim, Mingyang Li, and Ming Jen Tan. 2022. "Creating Functionally Graded Concrete Materials with Varying 3D Printing Parameters." *Virtual and Physical Prototyping* 17(3):662–81. doi:10.1080/17452759.2022.2048521;WGROUP:STRING:PUBLICATION.

28. Tcherniak, Dmitri. 2002. "Topology Optimization of Resonating Structures Using SIMP Method." *International Journal for Numerical Methods in Engineering* 54(11):1605–22. doi:10.1002/NME.484;WGROUP:STRING:PUBLICATION.

29. Tsavdaridis, Konstantinos Daniel. 2015. "Applications of Topology Optimization in Structural Engineering: High-Rise Buildings and Steel Components." *Jordan Journal of Civil Engineering* 9(3):335–57. doi:10.14525/JJCE.9.3.3076.

30. Tyflopoulos, Evangelos, and Martin Steinert. 2022. "A Comparative Study of the Application of Different Commercial Software for Topology Optimization." *Applied Sciences (Switzerland)* 12(2):611. doi:10.3390/APP12020611/S1.

31. Vantyghem, Gieljan, Wouter De Corte, Emad Shakour, and Oded Amir. 2020. "3D Printing of a Post-Tensioned Concrete Girder Designed by Topology Optimization." *Automation in Construction* 112:103084. doi:10.1016/J.AUTCON.2020.103084.

32. Wang, Qiang, Wenwei Yang, Li Wang, Gang Bai, and Guowei Ma. 2025. "Reinforcement Design and Structural Performance for the Topology Optimized 3D Printed Concrete Truss Beams." *Engineering Structures* 332:120064. doi:10.1016/J.ENGSTRUCT.2025.120064.

33. Wang, Xianggang, Lutao Jia, Zijian Jia, Chao Zhang, Yuning Chen, Lei Ma, Zhibin Wang, Zhicong Deng, Nemkumar Banthia, and Yamei Zhang. 2022. "Optimization of 3D Printing Concrete with Coarse Aggregate via Proper Mix Design and Printing Process." *Journal of Building Engineering* 56:104745. doi:10.1016/J.JOBE.2022.104745.

34. Xiong, Baocheng, Ping Nie, Huanbao Liu, Xiaoxi Li, Zihan Li, Wenyu Jin, Xiang Cheng, Guangming Zheng, and Liang Wang. 2024. "Optimization of Fiber Reinforced Lightweight Rubber Concrete Mix Design for 3D Printing." *Journal of Building Engineering* 88:109105. doi:10.1016/J.JOBE.2024.109105.

35. Yi, Sinan, Gengdong Cheng, and Liang Xu. 2016. "Stiffness Design of Heterogeneous Periodic Beam by Topology Optimization with Integration of Commercial Software." *Computers & Structures* 172:71–80. doi:10.1016/J.COMPSTRUC.2016.05.012.

36. Zhu, Ji Hong, Wei Hong Zhang, and Liang Xia. 2015. "Topology Optimization in Aircraft and Aerospace Structures Design." *Archives of Computational Methods in Engineering 2015 23:4* 23(4):595–622. doi:10.1007/S11831-015-9151-2.

37. Zuo, Zhi Hao, and Yi Min Xie. 2015. "A Simple and Compact Python Code for Complex 3D Topology Optimization." *Advances in Engineering Software* 85:1–11. doi:10.1016/J.ADVENGSOFT.2015.02.006.